

Why Adopting Regularization and Normalization For Generative Adversarial Networks: A Survey

Ziqiang Li, Xintian Wu, Rentuo Tao, Pengfei Xia, Huanhuan Chen[†], *Senior Member, IEEE*, Bin Li[†], *Member, IEEE*

Abstract—Generative Adversarial Networks (GANs) have been widely applied in different scenarios thanks to the development of deep neural networks. The proposal of original GAN is based upon the non-parametric assumption of the infinite capacity of networks. It is still unknown whether GANs can generate realistic samples without any prior information. Due to the overconfident assumption, many issues need to be addressed in GANs' training, such as non-convergence, mode collapses, gradient vanishing, overfitting, discriminator forgetting, and the sensitivity of hyperparameters. As acknowledged, regularization and normalization are common methods of introducing prior information that can be used for stabilizing training and improving discrimination. At present, many regularization and normalization methods are proposed in GANs. However, as far as we know, there is no existing survey that has particularly focused on the systematic purposes and developments of these solutions. In this work, we perform a comprehensive survey of the regularization and normalization technologies from different perspectives of GANs training. First, we systematically and comprehensively describe the different perspectives of GANs training and thus obtain the different purposes of regularization and normalization in GANs training. In accordance with the different purposes, we propose a new taxonomy and summary a large number of existing studies. Furthermore, we compare the performance of the mainstream methods on different datasets fairly and investigate the regularization and normalization technologies that have been frequently employed in SOTA GANs. Finally, we highlight the possible future studies in this area.

Index Terms—Generative Adversarial Networks (GANs), Regularization, Normalization, Survey, Lipschitz

I. INTRODUCTION

GENERATIVE adversarial networks (GANs) [1] have been widely used in computer vision, such as image inpainting [2]–[4], style transfer [5]–[8], text-to-image translations [9]–[11], and attribute editing [12]–[15]. GANs training is a two-player zero-sum game between a generator and a discriminator, which can be understood by different perspectives:

This paper was submitted on November 16, 2020. This work was partially supported by National Natural Science Foundation of China under grand No.U19B2044, No.61836011 and No.91746209.

Ziqiang Li, Rentuo Tao, and Pengfei Xia are with the CAS Key Laboratory of Technology in Geo-spatial Information Processing and Application Systems, University of Science and Technology of China, Anhui, China. (E-mail: iceli, trtmelon, xpengfei@mail.ustc.edu.cn)

Xintian Wu is with computer science and technology, Zhejiang University. (Email:hsintien@zju.edu.cn)

Huanhuan Chen (Corresponding author) is with the School of Computer Science and Technology, University of Science and Technology of China, Anhui, China. (E-mail: hchen@ustc.edu.cn)

Bin Li (Corresponding author) is with the CAS Key Laboratory of Technology in Geo-spatial Information Processing and Application Systems, University of Science and Technology of China, Anhui, China. (E-mail: binli@ustc.edu.cn)

(i) "Making sample real" [1], [16], (ii) "Fitting distribution" [17], [18], and (iii) "Training dynamics" [19], [20]. From the different perspectives of GANs, there are many problems during GANs training, including non-convergence [21], [22], mode collapses [23], gradient vanishing [24], overfitting [25], discriminator forgetting [26] and deficiency [27], and the sensitivity of hyperparameters [28]. Many solutions to mitigate these issues have been proposed, focusing on designing new architectures [29], [30], new loss functions [18], [26], [31], [32], and new optimization methods [20], [30].

Different from the above methods, regularization and normalization discussed in this paper are compatible with different loss functions, model structures, and tasks. Regularization and normalization are widely applied in supervised tasks. Specifically, regularization is proposed to introduce prior information during the training of neural networks and provides many advantages, such as overfitting prevention [33], [34], semi-supervised assumptions [35], manifold assumptions [36], [37], feature selection [38], and low rank representation [39]. Furthermore, normalization [40], [41] is advantageous for the Stochastic Gradient Descent (SGD) [42], accelerating convergence and improving accuracy. Unlike the icing on the cake of supervisory tasks, regularization and normalization are utilized inevitably in weak-supervised and unsupervised tasks. GANs' training is a two-player zero-sum game solving Nash equilibrium and the proposal of standard GAN is based upon the non-parametric assumption of the infinite capacity of networks, which can be considered as an unsupervised task. Likewise, a growing body of works from different perspectives of GANs training demonstrate that unconstrained training of GANs may cause unstable training (generator [43] and discriminator [31]) and significant bias between real images and fake images (attributes domain [44] and frequency domain [27], [45]). Specifically, Jacobi regularization [19] needs to be used to achieve local convergence from the perspective of "Training dynamic"; Gradient penalty [31], weight normalization [46], and weight regularization need to be used to fulfill Lipschitz continuity and stabilize training from the perspective of "Fitting distribution"; Data augmentation [47] and preprocessing [45], consistency regularization [48], and self-supervision [26] need to be used to mitigate overfitting and improve discrimination from the perspective of "Making sample real". Therefore, advanced regularization and normalization techniques with rich assumptions are indispensable for GANs training.

Regularization and normalization are proved to be a simple and effective way to stabilize training and improve the perfor-

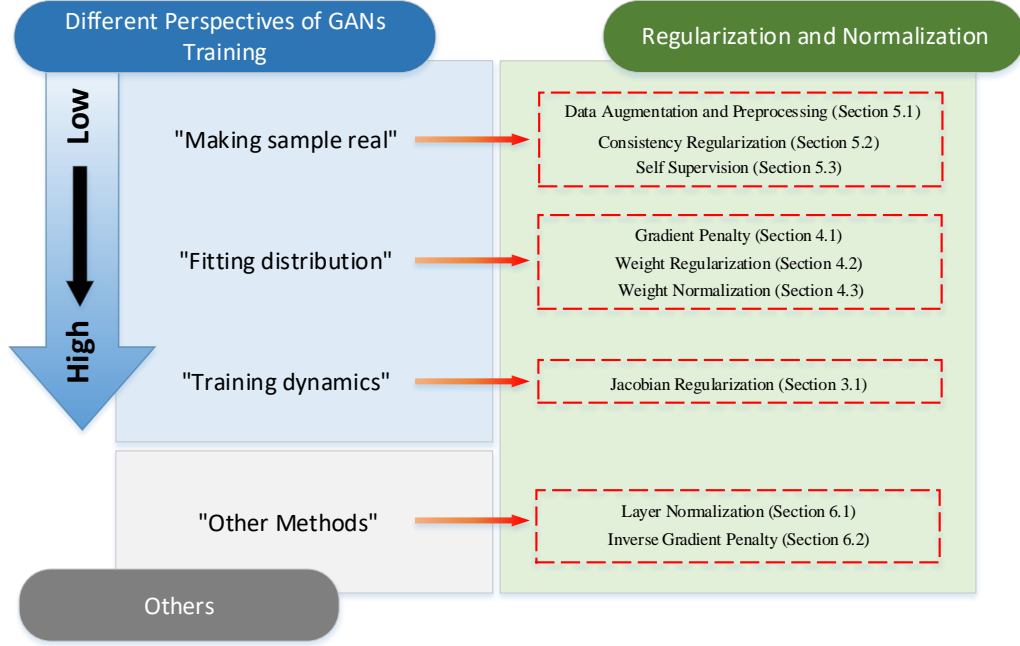


Fig. 1: The summary of the regularization and normalization for GANs.

mance of GANs in some literature [31], [49], [50]. As far as we know, there are few systematic surveys on this topic. To be more specific, some studies [28], [51] only summarize and analyze several popular methods which lack comprehensive coverage of this topic, whereas some other studies lack the detailed background, theoretical analysis, and description [52]. Moreover, the purposes and correlations of different methods are not presented comprehensively in these studies. In this paper, based on the different perspectives of GANs training, we propose a new taxonomy, denoted as **"Training dynamic"**, **"Fitting distribution"**, **"Making sample real"**, and **"Other methods"**, to enhance the understanding of regularization and normalization during the GANs training. The visual overview can be summarized in Fig.1. Furthermore, we also divide each group into different categories based on different forms of implementation. Specifically, Due to non-convexity, the global convergence is hard to achieve during GANs' training. Hence, some **Jacobian regularization** methods have been proposed to achieve local convergence in **"Training dynamic"**; **Gradient penalty**, **weight normalization**, and **weight regularization** can be used to fulfill Lipschitz continuity and ensure training stability of discriminator in **"Fitting distribution"**; **Data augmentation and preprocess**¹, **consistency regularization**, and **self-supervision** are proposed to mitigate overfitting and improve discrimination by introducing additional supervised information and data in **"Making sample real"**; Finally, **"Other methods"** contains **layer normalization** and **inverse**

gradient penalty, which are used for conditional generation and easing mode collapse, respectively

The rest of this paper is organized as follows: Section 2 introduces the background and different training perspectives of GANs. Section 3, 4, 5, and 6 describe many regularization and normalization methods in different groups, respectively. Furthermore, we investigate the regularization and normalization technologies that have been frequently employed in SOTA GANs in Section 7 and discuss the current problems and prospects for future work in Section 8.

II. BACKGROUND AND THREE PERSPECTIVES OF GANs TRAINING

GANs are two-player zero-sum games, where generator (G) and discriminator (D) try to optimize opposing loss functions to find the global Nash equilibrium. In general, GANs can be formulated as follows:

$$\min_{\phi} \max_{\theta} f(\phi, \theta) = \min_{\phi} \max_{\theta} \mathbb{E}_{x \sim p_r} [g_1(D_{\theta}(x))] + \mathbb{E}_{z \sim p_z} [g_2(D_{\theta}(G_{\phi}(z)))], \quad (1)$$

where ϕ and θ are parameters of the generator G and the discriminator D , respectively. p_r and p_z represent the real distribution and the latent distribution, respectively.

In this section, we first introduce the background of the regularization and prior. Furthermore, we elaborate the training of GANs from three perspectives: low level: the perspective of **"Making sample real"**, middle level: the perspective of **"Fitting distribution"**, and high level: the perspective of **"Training dynamic"**.

¹Data augmentation and preprocess introduce additional data and prior, which is similar to regularization. More importantly, both consistency regularization and self-supervision need different data transformation operations. Hence, this paper also discusses some works on this.

A. Regularization and Prior

Regularization is a technique to control the complexity of learning models. It has been widely used in learning models. Weight decay [53] is a typical method to minimize the square of weights together with the training loss in the training of neural networks [54], [55], which can be used to improve generalization. In Bayesian learning methods, regularization is termed as prior distribution, such as relevance vector machine [56], probabilistic classification vector machines [57], [58], and others [59]. Specifically, L2 regularization [34] is equivalent to introducing Gaussian prior to the parameters, and L1 regularization [33] is equivalent to introducing Laplace prior to the parameters. The theoretical connection between regularization and prior information has been investigated in neural network ensembles research [60], [61]. Regularization can not only control overfitting but also provide other characteristics like semi-supervised assumptions [35], manifold assumptions [36], [37], feature selection [38], low rank representation [39], [62], and consistency assumptions [48], [63].

B. Low Level: The Perspective of "Making sample real"

In this level, GANs can be considered as "counterfeiters-police" competition, where the generator (G) can be thought of counterfeiters, trying to produce fake currency and use it undetected, while the discriminator (D) is analogous to the police, trying to detect the counterfeit currency. This competition drives both teams to upgrade their methods until the fake currency is indistinguishable from the real ones. Generally, D estimates the real probability of both real and fake samples, which is very similar to the bi-classification task, while G generates fake samples similar to real ones. Hence, the loss function in Eq (1) can be formulated as:

$$\min_{\phi} \max_{\theta} f(\phi, \theta) = \min_{\phi} \max_{\theta} \mathbb{E}_{x \sim p_r} [\log(D_{\theta}(x))] + \mathbb{E}_{z \sim p_z} [\log(1 - D_{\theta}(G_{\phi}(z)))], \quad (2)$$

where $f(\phi, \theta)$ is a binary cross-entropy function, commonly used in binary classification problems. Eq (2) is proposed in original GAN [1] and can be optimized by alternate training. The training of discriminator is:

$$\max_{\theta} \mathbb{E}_{x \sim p_r} [\log(D_{\theta}(x))] + \mathbb{E}_{z \sim p_z} [\log(1 - D_{\theta}(G_{\phi}(z)))], \quad (3)$$

which is the same as a bi-classification task between real images and generated images. Hence, we can apply some techniques used in the classification task, such as new loss functions and some regularization methods, to the training of discriminator. Specifically, to overcome the gradients vanishing problem, Mao et al. [16] propose the LSGANs which adopts the least squares loss function for the discriminator. The least squares loss function can move the fake samples toward the decision boundary even though they are correctly classified. Based on this property, LSGANs are able to generate samples that are closer to real ones. Then the loss functions of LSGANs can be defined as follows:

$$\begin{aligned} \min_{\theta} \mathbb{E}_{x \sim p_r} [(D_{\theta}(x) - b)^2] + \mathbb{E}_{z \sim p_z} [(D_{\theta}(G_{\phi}(z)) - a)^2], \\ \min_{\phi} \mathbb{E}_{z \sim p_z} [(D_{\theta}(G_{\phi}(z)) - c)^2], \end{aligned} \quad (4)$$

where b and a are values that D for the training of real and fake samples respectively, c denotes the value that G wants D to believe for fake sample. Gradients vanishing problem of the LSGANs only appears with $D_{\theta}(G_{\phi}(z)) = c$, which is hard. Furthermore, Lin et al. [64] use SVM separating hyperplane that maximizes the margin. They use the Hinge loss to train the models, which can be formulated as:

$$\begin{aligned} \min_{\theta} \mathbb{E}_{x \sim p_r} [(1 - D_{\theta}(x))_+] + \mathbb{E}_{z \sim p_z} [1 + D_{\theta}(G_{\phi}(z))_+], \\ \min_{\phi} -\mathbb{E}_{z \sim p_z} D_{\theta}(G_{\phi}(z)), \end{aligned} \quad (5)$$

where $[x]_+ = \max\{0, x\}$.

The motivation of GANs is to train the generator based on the output of the discriminator. Unlike the direct training objective of the classification task (Minimizing cross-entropy loss), the objective of generator is indirect (With the help of the discriminator output). Hence, discriminator should provide a richer representation on the truth or false of samples compared to the classification task. More prior information and additional supervision tasks are urgent during the training process of the discriminator. Based on these, some regularization methods, such as **data augmentation and preprocessing**, **consistency regularization**, and **self-supervision** are proposed to improve the stability and generalizability [65] of discriminator.

C. Middle Level: The Perspective of "Fitting distribution"

At this level, generator $G(z)$ is considered as a distribution mapping function that maps latent distribution z to generated distribution $P_g(x)$, and the discriminator $D(x)$ is a distribution distance that evaluates the distance between the target distribution $P_r(x)$ and the generated distribution $P_g(x)$. The framework can be illustrated in Fig.2. For the optimal discriminator, the generator $G(z)$ tries to minimize the distance between $P_r(x)$ and $P_g(x)$. Specifically, generator of the vanilla GAN² [1] and f -GAN³ [17] can be considered to minimize Jensen-Shannon (JS) divergence and f divergence³, respectively. When the conditions of LSGANs loss are set to $b - c = 1$ and $b - a = 2$, the generator of the LSGAN can be considered to minimize the Pearson χ^2 divergence. Also, generator of the WGAN-div⁴ [66] and GAN-QP [67] can be considered to minimize the Wasserstein divergence and Quadratic divergence, respectively. For the GANs that is defined by Eq (1), Different choices of $g_1(t)$ and $g_2(t)$ lead to different GAN models. Specifically, vanilla GAN [1] can be described with $g_1(t) = g_2(-t) = -\log(1 + e^{-t})$, f -GAN [17] and WGAN [18] can be written as $g_1(t) = -e^{-t}$, $g_2(t) = 1 - t$ and $g_1(t) = g_2(-t) = t$, respectively.

²Vanilla GAN, also known as standard GAN, is the first GAN model.

³ f -GAN is a collective term for a type of GAN models whose discriminator minimizes f divergence. f divergence is the general form of KL divergence. It can be demonstrated as: $D_f(P||Q) = \int q(x) f(\frac{p(x)}{q(x)}) dx$, where f is a mapping function from non-negative real numbers to real numbers ($\mathbb{R}^+ \rightarrow \mathbb{R}$) that satisfies: (1) $f(1) = 0$. (2) f is a convex function. To be more specific, KL divergence corresponds to $f(u) = u \log u$ and JS divergence corresponds to $f(u) = -\frac{u+1}{2} \log \frac{1+u}{2} + \frac{u}{2} \log u$. More details can be viewed in [17]

⁴Different from WGAN-div, WGAN [18] minimize Wasserstein distance, not Wasserstein divergence.

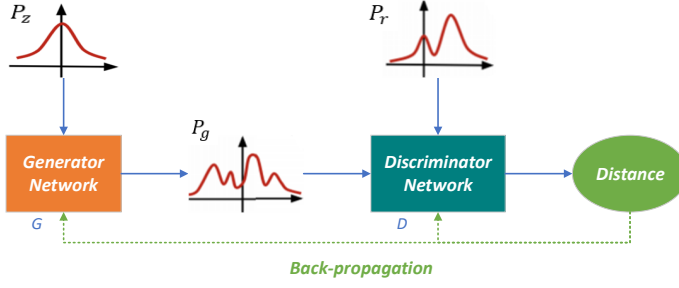


Fig. 2: The framework of GANs. P_z is a latent space distribution, P_r and P_g represent the real distribution and the generated distribution, respectively.

Generator is a transportation map from z to $p_g(x)$. In this section, we introduce the optimal transport and the optimal transport with regular term, which can lead to the form of Wasserstein GANs with gradient penalty [31] (WGAN-GP) and Wasserstein GANs with Lipschitz penalty [49] (WGAN-LP), respectively. Wasserstein distance is the most popular distance in GANs and it corresponds to the optimal transport of the generator. To solve the dual problem of Wasserstein distance, Lipschitz continuity is introduced, which is the reason why gradient penalty and weight normalization technologies are proposed in the GANs training. The following is a more detailed description.

Optimal transport [68] was proposed in the 18th century to minimize the transportation cost while preserving the measure quantities. Given the space with probability measures (X, μ) and (Y, ν) , if there is a map $T : X \rightarrow Y$ which is measure-preserving, then for any $B \subset Y$, having:

$$\int_{T^{-1}(B)} d\mu(x) = \int_B d\nu(y). \quad (6)$$

Writing the measure-preserving map as $T_*(\mu) = \nu$. For any $x \in X$ and $y \in Y$, the transportation distance can be defined as $c(x, y)$, then the total transportation cost is given by:

$$C(T) := \int_X c(x, T(x)) d\mu(x). \quad (7)$$

In the 18th century, Monge proposed the Optimal Mass Transportation Map that corresponds to the smallest total transportation cost: $C(T)$. The transportation cost corresponding to the optimal transportation map is called the Wasserstein distance between probability measures μ and ν :

$$W_c(\mu, \nu) = \min_T \left\{ \int_X c(x, T(x)) d\mu(x) \mid T_*(\mu) = \nu \right\}. \quad (8)$$

In 1940s, Kantorovich proved the existence and uniqueness of the solution for Monge problem [69], and according to the duality of linear programming, he obtained the Kantorovich-Rubinstein (KR) duality of Wasserstein distance:

$$W_c(\mu, \nu) = \max_{\varphi, \psi} \left\{ \int_X \varphi d\mu + \int_Y \psi d\nu \mid \varphi(x) + \psi(y) \leq c(x, y) \right\}. \quad (9)$$

This dual problem is constrained, defining the c -transform: $\psi(y) = \varphi^c(y) := \inf_x \{c(x, y) - \varphi(x)\}$, and the Wasserstein distance becomes:

$$W_c(\mu, \nu) = \max_{\varphi} \left\{ \int_X \varphi d\mu + \int_Y \varphi^c d\nu \right\}, \quad (10)$$

where φ is called the Kantorovich potential. It can be shown that if $c(x, y) = |x - y|$ and Kantorovich potential satisfies the 1-Lipschitz continuity, then $\varphi^c = -\varphi$. At this time, Kantorovich potential can be fitted by a deep neural network, which is recorded as φ_ξ . Wasserstein distance is:

$$W_c(\mu, \nu) = \max_{\|\varphi_\xi\|_L \leq 1} \left\{ \int_X \varphi_\xi d\mu - \int_Y \varphi_\xi d\nu \right\}. \quad (11)$$

If X is the generated image space, Y is the real sample space, Z is latent space and g_θ is the generator, then the Wasserstein GANs (WGAN) can be formulated as a min-max problem:

$$\min_{\theta} \max_{\|\varphi_\xi\|_L \leq 1} \left\{ \int_Z \varphi_\xi(g_\theta(z)) dz - \int_Y \varphi_\xi(y) dy \right\}. \quad (12)$$

In the optimization process, the generator and the Kantorovich potential function (discriminator) are independent of each other, which can be optimized in a step-by-step iteration.

If $c(x, y) = \frac{|x - y|^2}{2}$, there is a convex function u that is called Brenier potential [70]. The optimal transportation map is given by the gradient map of Brenier potential: $T(x) = \nabla u(x)$. There exists a relationship between Kantorovich potential and Brenier potential [71]:

$$u(x) = \frac{|x|^2}{2} - \varphi(x). \quad (13)$$

From the previous discussion, we know that the optimal transportation map (Brenier potential) corresponds to the generator, and Kantorovich potential corresponds to the discriminator. After the discriminator is optimized, the generator can be directly derived without having to go through the optimization process [71].

The transportation cost of Eq (3) can be defined as the form of two distribution distances:

$$OT(P||Q) = \inf_{\pi} \int \pi(x, y) c(x, y) dx dy, \quad (14)$$

where $\pi(x, y)$ is the joint distribution, satisfying $\int_y \pi(x, y) dy = P(x)$ and $\int_x \pi(x, y) dx = Q(y)$. The dual form of Eq (10) is derived as follows:

$$OT(P||Q) = \max_{\varphi, \psi} \left\{ \int_X \varphi(x) P(x) dx + \int_Y \psi(y) Q(y) dy \mid \varphi(x) + \psi(y) \leq c(x, y) \right\}. \quad (15)$$

Considering the optimal transportation with regular terms, Peyré et al. [72] added the entropic regularization for optimal transportation that transforms the dual problem into a smooth unconstrained convex problem. The regularized optimal transport is defined as:

$$OT_c(P||Q) = \min_{\pi} \int \pi(x, y) c(x, y) dx dy + \epsilon E(\pi). \quad (16)$$

If $E(\pi) = \int_x \int_y \pi(x, y) \log\left(\frac{\pi(x, y)}{P(x)Q(y)}\right) dx dy$, Eq (12) can be written as:

$$\begin{aligned} OT_c(P||Q) &= \min_{\pi} \int \pi(x, y) c(x, y) dx dy + \\ &\quad \epsilon \int_x \int_y \pi(x, y) \log\left(\frac{\pi(x, y)}{P(x)Q(y)}\right) dx dy \quad (17) \\ s.t. \quad \int_y \pi(x, y) dy &= P(x), \int_x \pi(x, y) dx = Q(y). \end{aligned}$$

The dual form of Eq (13) becomes:

$$\begin{aligned} OT_c(P||Q) &= \max_{\varphi, \psi} \int_x \varphi(x) P(x) dx + \int_y \psi(y) Q(y) dy \\ &\quad + \frac{\epsilon}{e} \int_x \int_y \exp\left(\frac{-(c(x, y) + \varphi(x) + \psi(y))}{\epsilon}\right) dx dy. \quad (18) \end{aligned}$$

This section introduces the optimal transportation and optimal transportation with regular terms, based on which the form of WGAN can be achieved and the important condition, Lipschitz continuity, is also proposed. As acknowledged, **gradient penalty** is a sample and effective way to implement the Lipschitz continuity.

D. Lipschitz Continuity and Matrix Norm

WGAN is the most popular generative adversarial network. From the optimal transport in the last subsection, to obtain Eq (11), the discriminator must satisfy the 1-Lipschitz continuity. This section introduces the form of the Lipschitz constant and shows that the spectral norm and the Lipschitz constant have the same meaning.

1-Lipschitz continuity can be represented as:

$$||D(x_1) - D(x_2)|| \leq ||x_1 - x_2||.^5 \quad (19)$$

Generally, considering the K-Lipschitz for a neural network $f(x)$:

$$f(x) = g_N \circ \dots \circ g_2 \circ g_1(x),^6 \quad (20)$$

where $g_i(x) = \sigma(W_i x + b_i)$. And K-Lipschitz continuity for $f(x)$ is:

$$||f(x_1) - f(x_2)|| \leq K ||x_1 - x_2||, \quad (21)$$

where K is Lipschitz constant of the function f . Due to the consistency of Lipschitz $||h \circ g||_{Lip} \leq ||h||_{Lip} \cdot ||g||_{Lip}$, g_i needs to satisfy the C-Lipschitz continuity ($C = \sqrt[K]{K}$) so that f can satisfy the K-Lipschitz continuity:

$$||g_i(x_1) - g_i(x_2)|| \leq C ||x_1 - x_2||, \quad (22)$$

$$||\sigma(Wx_1 + b) - \sigma(Wx_2 + b)|| \leq C ||x_1 - x_2||. \quad (23)$$

When $x_1 \rightarrow x_2$, the Taylor expansion of Eq (19):

$$||\frac{\partial \sigma}{\partial x} W(x_1 - x_2)|| \leq C ||x_1 - x_2||. \quad (24)$$

⁵Lipschitz continuity can be defined by any form of norm.

⁶ \circ is the symbol for function cascade. Specifically, $h \circ g(x) = h(g(x))$. This definition of neural network is not general, such as DenseNet [73] and ResNet [74], which can not be defined like this. Therefore, we do not strictly derive the relationship between the matrix norm and Lipschitz continuity.

Normally, σ is a function with limited derivatives such as Sigmoid, so the C'-Lipschitz continuity can be written as:

$$||W(x_1 - x_2)|| \leq C' ||x_1 - x_2||, \quad (25)$$

where C' is a limited constant, which is determined by $\frac{\partial \sigma}{\partial x}$ and C. Similarly, the spectral norm of matrix is defined by:

$$||W||_2 = \max_{x \neq 0} \frac{||Wx||}{||x||}. \quad (26)$$

From now, the spectral norm $||W||_2$ can be used to represent the Lipschitz constant C' . The Lipschitz continuity can be achieved by normalizing the spectral norm of the weight, approximately. Hence, **weight normalization** and **weight regularization** can also be used to enable the Lipschitz continuity of the discriminator.

E. High Level: The Perspective of "Training dynamic"

GANs training is a two-player zero-sum game, which exists the Nash equilibrium solution. At this level, we analyze the convergence of GANs by understanding the optimization process. Based on these, some regularization technologies are proposed to guide the GANs model to reach the theoretical equilibrium point, and thus improve the effectiveness of GANs.

Reconsidering the Eq (1) in Section 2, the training of GANs is achieved by solving a two-player zero-sum game via Simultaneous Gradient Descent (SimGD) [1], [18]. The updates of the SimGD are given as:

$$\begin{aligned} \phi^{(k+1)} &= \phi^{(k)} - h \nabla_{\phi} f(\phi^{(k)}, \theta^{(k)}), \\ \theta^{(k+1)} &= \theta^{(k)} + h \nabla_{\theta} f(\phi^{(k)}, \theta^{(k)}). \end{aligned} \quad (27)$$

Assuming that the objectives of GANs are convex, many research works discussed their global convergence characteristics [17], [75]. However, due to the high non-convexity of deep networks, even a simple GAN does not satisfy the convexity assumption [76]. A recent study [77] shows that it is unrealistic to obtain approximate global convergence under the assumption of the optimal discriminator, so the community considers local convergence. It hopes that the trajectory of the dynamic system can enter a local convergence point with continuity iterations, that is, Nash equilibrium:

$$\begin{aligned} \bar{\phi} &= \arg \max_{\phi} -f(\phi, \bar{\theta}), \\ \bar{\theta} &= \arg \max_{\theta} f(\bar{\phi}, \theta). \end{aligned} \quad (28)$$

If the point $(\bar{\phi}, \bar{\theta})$ is called the local Nash-equilibrium, Eq (28) holds in a local neighborhood of $(\bar{\phi}, \bar{\theta})$. For this differentiable two-player zero-sum games, a vector is defined as below:

$$v(\phi, \theta) = \begin{pmatrix} -\nabla_{\phi} f(\phi, \theta) \\ \nabla_{\theta} f(\phi, \theta) \end{pmatrix}. \quad (29)$$

The Jacobian matrix is:

$$v'(\phi, \theta) = \begin{pmatrix} -\nabla_{\phi, \phi}^2 f(\phi, \theta) & -\nabla_{\phi, \theta}^2 f(\phi, \theta) \\ \nabla_{\theta, \phi}^2 f(\phi, \theta) & \nabla_{\theta, \theta}^2 f(\phi, \theta) \end{pmatrix}. \quad (30)$$

Lemma 2.1: For zero-sum games, v' is negative semi-definite for any local Nash-equilibrium. Conversely, if $v(\bar{x}) = 0$ and v' is negative definite, then \bar{x} is a local Nash-equilibrium.

Proof 2.1: Refer to [19] \square

Lemma 2.1 [19] gives the conditions for the local convergence of GANs, which is converted into the negative semi-definite problem of the Jacobian matrix. Negative semi-definite of the Jacobian matrix corresponds to its eigenvalue less than or equal to 0. If the eigenvalue of the Jacobian matrix at a certain point is a negative real number, the training process can converge; but if the eigenvalue is complex and the real part of the eigenvalue is small and the imaginary part is relatively large, the training process is difficult to converge unless the learning rate is very small.

Proposition 2.2: Let $F : \Omega \rightarrow \Omega$ be a continuously differentiable function on an open subset Ω of \mathbb{R}^n and let $\bar{x} \in \Omega$ be so that:

1. $F(\bar{x}) = \bar{x}$ and
2. the absolute values of the eigenvalues of the Jacobian $F'(\bar{x})$ are all smaller than 1.

There is an open neighborhood U of \bar{x} so that for all $x_0 \in U$, the iterates $F^{(k)}(x_0)$ converge to \bar{x} . The rate of convergence is at least linear. More precisely, the error $\|F^{(k)}(x_0) - \bar{x}\|$ is in $O(|\lambda_{\max}|^k)$ for $k \rightarrow \infty$ where λ_{\max} is the eigenvalue of $F'(\bar{x})$ with the largest absolute value.

Proof 2.2: Refer to Section 3 in [19] and Proposition 4.4.1 in [78]. \square

From Proposition 2.2: Under the premise of asymptotic convergence, the local convergence of GAN is equivalent to the absolute value of all eigenvalues of the Jacobian matrix at the fixed point ($v(\bar{\phi}, \bar{\theta}) = 0$) being less than 1. To get this condition, some **Jacobian regularization** [19], [79]–[81] need to be used.

III. REGULARIZATION AND NORMALIZATION OF "TRAINING DYNAMIC"

Assuming the objectives of GANs are convex-concave, some works have provided the global convergence of GANs [17], [82]. However, these theoretical convergence analyses can only be applied to the GANs with existing the optimal discriminator. It is not capable to achieve the optimal discriminator, thus, more works focus on analyzing the local convergence of GANs. According to Nagarajan et al. [79] and Mescheder et al. [19], under some assumptions, GANs dynamics are locally convergent. However, if these assumptions are not satisfied, especially if the data distributions are not continuous, GANs dynamics can not always be locally convergent unless some regularization technologies are used.

Initially, **Jacobian regularization** technologies [19], [79], minimizing Jacobi matrix, are proposed to achieve local convergence. In this section, we survey these methods. Subsequently, Mescheder et al. [80] propose a simplified gradient penalties method, named zero-centered gradient penalties (z-GP), that guarantees the local convergence under suitable assumptions. Since it is similar to 0-GP, we will cover it in detail in Section 4.

A. Jacobian Regularization

In Proposition 2.2 of Section 2: absolute values of all eigenvalues of the Jacobian matrix of the $V(\phi, \theta)$ are expected to be less than 1 at the fixed point, which is equivalent to the real part of the eigenvalue being negative. Additionally, the learning rate must be relatively low [19]. To meet these requirements, Mescheder et al. [19] used the Consensus Optimization (ConOpt) to make the real part of the eigenvalue negative. Its regularized updates are:

$$\begin{aligned}\phi^{(k+1)} &= \phi^{(k)} + h \nabla_{\phi} \left(-f(\phi^{(k)}, \theta^{(k)}) - \gamma L(\phi^k, \theta^k) \right), \\ \theta^{(k+1)} &= \theta^{(k)} + h \nabla_{\theta} \left(f(\phi^{(k)}, \theta^{(k)}) - \gamma L(\phi^k, \theta^k) \right),\end{aligned}\quad (31)$$

where $L(\phi^k, \theta^k) = \frac{1}{2} \|\nabla_{\phi} f(\phi^k, \theta^k)\|^2 + \frac{1}{2} \|\nabla_{\theta} f(\phi^k, \theta^k)\|^2$ is the regularization of the Jacobian matrix.

Apart from Mescheder et al, Nagaraja et al. [79] also analyze the relationship between local convergence of GANs and all eigenvalues of the Jacobian of the gradient vector field. They prove the local convergence for absolutely continuous generator and data distributions under certain regularity assumptions. This requires the loss function of the GANs to be strictly concave, which is not the case for some GANs. Based on this, a simple regularization technology that regularized the generator using the gradient of the discriminator is proposed by Nagaraja et al. [79]. The regularized updates for the generator can be expressed as:

$$\phi^{(k+1)} = \phi^{(k)} - h \nabla_{\phi} f(\phi^{(k)}, \theta^{(k)}) - \frac{1}{2} h \gamma \nabla_{\phi} \|\nabla_{\theta} f(\phi^k, \theta^k)\|^2. \quad (32)$$

Herein, the update of the discriminator is similar to SimGD. Furthermore, Nie et al. [76] propose a method that only regularizes the discriminator. The regularized update of the discriminator in this case is given by:

$$\theta^{(k+1)} = \theta^{(k)} + h \nabla_{\theta} f(\phi^{(k)}, \theta^{(k)}) - \frac{1}{2} h \gamma \nabla_{\theta} \|\nabla_{\phi} f(\phi^k, \theta^k)\|^2. \quad (33)$$

The update of the generator is the same as SimGD. Nie et al. [76] propose JAcobian REgularization (JARE) that regularizes both the generator and the discriminator. The regularized updates for the generator and the discriminator are:

$$\begin{aligned}\phi^{(k+1)} &= \phi^{(k)} - h \nabla_{\phi} f(\phi^{(k)}, \theta^{(k)}) - \frac{1}{2} h \gamma \nabla_{\phi} \|\nabla_{\theta} f(\phi^k, \theta^k)\|^2, \\ \theta^{(k+1)} &= \theta^{(k)} + h \nabla_{\theta} f(\phi^{(k)}, \theta^{(k)}) - \frac{1}{2} h \gamma \nabla_{\theta} \|\nabla_{\phi} f(\phi^k, \theta^k)\|^2.\end{aligned}\quad (34)$$

The key difference between JARE and ConOpt is that JARE does not contain the Hessians $\nabla_{\phi, \phi}^2 f(\phi^k, \theta^k)$ and $\nabla_{\theta, \theta}^2 f(\phi^k, \theta^k)$ in the regularization term, which avoids two factors⁷ of the Jacobian in the GANs training dynamics simultaneously. (i) the Phase Factor, i.e., the Jacobian has complex eigenvalues with a large imaginary-to-real ratio; (ii) the Conditioning Factor, i.e., the Jacobian is ill-conditioned.

⁷Intuitively, a reason for not introducing Hessians is to avoid the risk of reversing the gradient flows, which may diverge the GAN training dynamics (see Appendix C in [76] for a detailed explanation).

The above discussions of local convergence during GANs training involve a premise: absolutely continuous data and generator distributions. Indeed, the assumption of absolute continuity is not true for common cases of GANs, where both distributions, specially the data distribution, may lie on lower-dimensional manifolds [83]. More generally, Mescheder et al. [80] extend the convergence proof by Nagaraja et al. [79] to the case where the generator and data distribution do not locally have the same support. Based on this, a simplified zero-centered gradient penalties (zc-GP) method is proposed, which guarantees the local convergence under suitable assumptions. Zc-GP is obtained from the training dynamic, which is similar to 0-GP methods mentioned in Section 4. We will cover it in detail in that section.

In summary, **Jacobian regularization** technologies are obtained from the training dynamic of GANs, which are used for achieving local convergence. The summary of the Jacobian regularization methods is demonstrated in Table I. From the form of the updating, Jacobian regularization is similar to the Gradient penalty. In general, zc-GP is used in many SOTA methods, which are demonstrated in Section 7.

IV. REGULARIZATION AND NORMALIZATION OF "FITTING DISTRIBUTION"

From the perspective of "Fitting distribution", generator is considered as a distribution mapping function and the optimal discriminator is considered to be the distribution distance. Among them, Wasserstein distance is the most popular in GANs and it corresponds to the optimal transport of the generator. To solve the dual problem of Wasserstein distance, Lipschitz continuity is introduced, which is the first time that Lipschitz continuity has been introduced into the training of GANs. The Wasserstein distance-based GANs (WGAN and WGAN-GP) have achieved remarkable results during the training. However, some works [21], [84], [85] suggest that the success of WGAN-GP is not due to the Wasserstein distance and the Lipschitz constraint of discriminator may improve the performance and stability of GANs training regardless of the statistical distance used as a loss function. Based on these, the Lipschitz continuity of discriminator is an essential condition during GANs training. As acknowledged, **gradient penalty**, **weight normalization**, and **weight regularization** are widely applied in GANs training for fulfilling Lipschitz continuity, which will be summarized at this section.

A. Gradient Penalty

Gradient penalty is a simple and direct way to fulfill Lipschitz continuity. Specifically, K-Lipschitz continuity (mentioned in Eq (21)) of the function f can be accessed by $\min_{\hat{x} \sim \pi} (\|\nabla f(\hat{x})\|_2 - K)^2$. According to the optimal transport theory mentioned in Section 2.3, gradient penalty can be used for the approximation of $W_c(\mu, \nu)$ (Eq (11)) in WGANs, named WGAN-GP [31]. Specifically, WGAN-GP fulfills the 1-Lipschitz continuity of the discriminator by $\min_{\hat{x} \sim \pi} (\|\nabla D_\theta(\hat{x})\|_2 - 1)^2$, which limits the gradient of the discriminator to 1. Although WGAN-GP solves the instability of GANs training to some extent, the assumption of optimal

transport is a constrained linear programming problem. Overly strict restriction reduces the exploratory of the discriminator.

In contrast, the optimal transport with the regular term mentioned in section 2.3 is an unconstrained optimization problem. Petzka et al. [49] set $c(x, y) = \|x - y\|_2$ in Eq (18), and the dual form of optimal transport with the regular term can be expressed as:

$$\sup_{\varphi, \psi} \{ \mathbb{E}_{x \sim p(x)} [\varphi(x)] - \mathbb{E}_{y \sim q(y)} [\psi(y)] - \frac{4}{\epsilon} \int \int \max\{0, (\varphi(x) - \psi(y) - \|x - y\|_2)\}^2 dp(x) dq(y) \}. \quad (35)$$

Similar to dealing with a single function, one can replace $\varphi = \psi$ in Eq (35), which leads to the objective of minimum:

$$\mathbb{E}_{y \sim q(y)} [\varphi(y)] - \mathbb{E}_{x \sim p(x)} [\varphi(x)] + \frac{4}{\epsilon} \int \int \max\{0, (\varphi(x) - \varphi(y) - \|x - y\|_2)\}^2 dp(x) dq(y). \quad (36)$$

Similar to optimal transport corresponds to 1-Lipschitz continuity, the optimal transport with the regular term corresponds to k-Lipschitz continuity ($k \leq 1$) of the discriminator, named WGAN-LP [49], which is implemented by $\min_{\hat{x} \sim \pi} [(\max\{0, \|\nabla D_\theta(\hat{x})\|_2 - 1\})^2]$. WGAN-LP with using a weaker regularization term enforcing the Lipschitz constraint of the discriminator achieves the preferable performance.

WGAN-GP and WGAN-LP introduce Wasserstein distance into GANs framework. Due to the gap between limited input samples and the strict Lipschitz constraint on the whole input sample domain, the approximate of the Wasserstein distance is challenging. To this end, WGAN-div [66] introduces a Wasserstein divergence into GANs training. The objective of WGAN-div can be smoothly derived as:

$$\mathbb{E}_{y \sim q(y)} [\varphi(y)] - \mathbb{E}_{x \sim p(x)} [\varphi(x)] + k \mathbb{E}_{\hat{x} \sim \pi} [\|\varphi(\hat{x})\|^P]. \quad (37)$$

The objective of WGAN-div is similar to WGAN-GP and WGAN-LP. It can be considered as achieving 0-Lipschitz continuity of discriminator by adopting $\min_{\hat{x} \sim \pi} [\|\nabla D_\theta(\hat{x})\|^P]$.

Generally, Wasserstein distance and Wasserstein divergence, reliable ways of measuring the difference between fake and real data distribution, lead to stable training of WGAN-based algorithms. However, recent work [84] shows that the c-transform method [93] achieves a much better estimation of Wasserstein divergence but obtains worse performance compared to the gradient penalty method. The results demonstrate that the success of WGAN-based methodologies can not in truth be attributed to approximate the Wasserstein distance and the gradient penalty methods improve the performance indeed. Furthermore, some works [21], [85], [94] also demonstrate that gradient penalty methods of discriminator, such as 1-GP, k-GP ($k \leq 1$), and 0-GP stabilize the training and improve the performance of GANs remarkably regardless of the loss functions. Based on these observations, stabilizing GANs training using gradient penalty is widely applied by the community for various losses of GANs. In the rest of this section, we will discuss gradient penalty methods regardless of the loss function and

TABLE I: The summary of the Jacobian regularization

Method	regularized updates of generator	regularized updates of discriminator
SimGD [1]	$\phi^{(k+1)} = \phi^{(k)} - h \nabla_{\phi} f(\phi^{(k)}, \theta^{(k)})$	$\theta^{(k+1)} = \theta^{(k)} + h \nabla_{\theta} f(\phi^{(k)}, \theta^{(k)})$
ConOpt [19]	$\phi^{(k+1)} = \phi^{(k)} - h \nabla_{\phi} f(\phi^{(k)}, \theta^{(k)}) - \frac{1}{2} h \gamma \nabla_{\phi} \ \nabla_{\theta} f(\phi^{(k)}, \theta^{(k)})\ ^2$	$\theta^{(k+1)} = \theta^{(k)} + h \nabla_{\theta} f(\phi^{(k)}, \theta^{(k)}) - \frac{1}{2} h \gamma \nabla_{\theta} \ \nabla_{\phi} f(\phi^{(k)}, \theta^{(k)})\ ^2$
Generator [79]	$\phi^{(k+1)} = \phi^{(k)} - h \nabla_{\phi} f(\phi^{(k)}, \theta^{(k)}) - \frac{1}{2} h \gamma \nabla_{\phi} \ \nabla_{\theta} f(\phi^{(k)}, \theta^{(k)})\ ^2$	$\theta^{(k+1)} = \theta^{(k)} + h \nabla_{\theta} f(\phi^{(k)}, \theta^{(k)})$
Discriminator [76]	$\phi^{(k+1)} = \phi^{(k)} - h \nabla_{\phi} f(\phi^{(k)}, \theta^{(k)})$	$\theta^{(k+1)} = \theta^{(k)} + h \nabla_{\theta} f(\phi^{(k)}, \theta^{(k)}) - \frac{1}{2} h \gamma \nabla_{\theta} \ \nabla_{\phi} f(\phi^{(k)}, \theta^{(k)})\ ^2$
JARE [76]	$\phi^{(k+1)} = \phi^{(k)} - h \nabla_{\phi} f(\phi^{(k)}, \theta^{(k)}) - \frac{1}{2} h \gamma \nabla_{\phi} \ \nabla_{\theta} f(\phi^{(k)}, \theta^{(k)})\ ^2$	$\theta^{(k+1)} = \theta^{(k)} + h \nabla_{\theta} f(\phi^{(k)}, \theta^{(k)}) - \frac{1}{2} h \gamma \nabla_{\theta} \ \nabla_{\phi} f(\phi^{(k)}, \theta^{(k)})\ ^2$
zc-GP [80]	$\phi^{(k+1)} = \phi^{(k)} - h \nabla_{\phi} f(\phi^{(k)}, \theta^{(k)})$	$\theta^{(k+1)} = \theta^{(k)} + h \nabla_{\theta} f(\phi^{(k)}, \theta^{(k)}) - \frac{1}{2} h \gamma \nabla_{\theta} \ \nabla D_{\theta}(x)\ ^2$

TABLE II: The Gradient penalty of the Discriminator. μ and ν are real and generated distribution, respectively.

Method	\mathcal{L}_{GP}	π	Lipschitz continuity
WGAN-GP [31]	$\mathbb{E}_{\hat{x} \sim \pi} (\ \nabla D_{\theta}(\hat{x})\ _2 - 1)^2$	$t \cdot p_r + (1-t) \cdot p_g$	$\ D_{\theta}\ _{Lip} \rightarrow 1$
DRAGAN [21]	$\mathbb{E}_{\hat{x} \sim \pi} (\ \nabla D_{\theta}(\hat{x})\ _2 - 1)^2$	$p_r + \epsilon$	$\ D_{\theta}\ _{Lip} \rightarrow 1$
Max-GP [86]	$\left(\max_{\hat{x} \sim \pi} \ \nabla D_{\theta}(\hat{x})\ _2 - 1 \right)^2$	$t \cdot p_r + (1-t) \cdot p_g$	$\ D_{\theta}\ _{Lip} \rightarrow 1$
ALP [87]	$\mathbb{E}_{\hat{x} \sim \pi} (\ \nabla D_{\theta}(\hat{x})\ _2 - 1)^2$	$p_r \cup p_g$	$\ D_{\theta}\ _{ALP-Lip} \rightarrow 1$
Banach-GP [88]	$\mathbb{E}_{\hat{x} \sim \pi} (\ \nabla D_{\theta}(\hat{x})\ _{B^*} - 1)^2$	$t \cdot p_r + (1-t) \cdot p_g$	$\ D_{\theta}\ _{Lip} \rightarrow 1$
WGAN-LP [49]	$\mathbb{E}_{\hat{x} \sim \pi} \left[(\max\{0, \ \nabla D_{\theta}(\hat{x})\ _2 - 1\})^2 \right]$	$t \cdot p_r + (1-t) \cdot p_g$	$\ D_{\theta}\ _{Lip} \leq 1$
SWGAN [89]	$\mathbb{E}_{\hat{x} \sim \pi} \left[(\max\{0, \ \nabla D_{\theta}(\hat{x})\ _2 - 1\})^2 \right]$	$t \cdot p_r + (1-t) \cdot p_g$	$\ D_{\theta}\ _{Lip} \leq 1$
zc-GP [66], [80], [90]	$\mathbb{E}_{\hat{x} \sim \pi} \ \nabla D_{\theta}(\hat{x})\ _2^2$	$p_r \cup p_g$	$\ D_{\theta}\ _{Lip} \rightarrow 0$
GAN-QP [67]	$\mathcal{L}_{GP} = \mathbb{E}_{x_r, x_g \sim \pi} \frac{(D_{\theta}(x_r) - D_{\theta}(x_g))^2}{\ x_r - x_g\ }$	$\pi = p_r \cdot p_g$	$\frac{(D_{\theta}(x_r) - D_{\theta}(x_g))^2}{\ x_r - x_g\ } \rightarrow 0$
ZP-Max [91]	$\max_{\hat{x} \sim \pi} \ \nabla D_{\theta}(\hat{x})\ _2^2$	$t \cdot p_r + (1-t) \cdot p_g$	$\ D_{\theta}\ _{Lip} \rightarrow 0$
ZP [92]	$\mathbb{E}_{\hat{x} \sim \pi} \ \nabla D_{\theta}(\hat{x})\ _2^2$	$t \cdot p_r + (1-t) \cdot p_g$	$\ D_{\theta}\ _{Lip} \rightarrow 0$

divide them into three parts: **1-GP**: $\min \mathbb{E}_{\hat{x} \sim \pi} (\|\nabla D_{\theta}(\hat{x})\| - 1)^p$, **k-GP** ($k \leq 1$): $\min \mathbb{E}_{\hat{x} \sim \pi} [(\max\{0, \|\nabla D_{\theta}(\hat{x})\| - 1\})^p]$, and **0-GP**: $\min \mathbb{E}_{\hat{x} \sim \pi} [\|\nabla D_{\theta}(\hat{x})\|^p]$, where π is the distribution of different image space (entire image space or part of image space) and $\|\cdot\|$ represents the norm of the gradient. Generally, the loss function of the discriminator with GP can be formulated as:

$$\mathcal{L}_D = f(\phi, \theta) + \lambda \mathcal{L}_{GP}, \quad (38)$$

where $f(\phi, \theta)$ is the uniform loss function defined in Eq (1) and \mathcal{L}_{GP} is the gradient penalty regularization.

1) **1-GP**: 1-GP is first applied by Gulrajani et al. [31] during the training of GANs, named WGAN-GP. WGAN-GP uses the 2-norm gradient penalty across the entire image domain, which can be formulated as:

$$\mathcal{L}_{GP} = \mathbb{E}_{\hat{x} \sim \pi} (\|\nabla D_{\theta}(\hat{x})\|_2 - 1)^2, \quad (39)$$

where π is the distribution of entire image space approximated by the interpolation of real distribution (p_r) and generated distribution (p_g): $\pi = t \cdot p_r + (1-t) \cdot p_g$ for $t \sim U[0, 1]$. Although, WGAN-GP stabilizes the training of GANs astonishingly, the overly strict gradient penalty limits the exploratory of discriminator. To loosen the penalty, many efforts of π , $\|\cdot\|$, and gradient direction are proposed.

For relaxing the image distribution, Kodali et al. [21] track the training process of GANs and find that the decrease of the Inception Score (IS) is accompanied by a sudden change of the discriminator's gradient around the real images. They propose

DRAGAN and only restrict the Lipschitz constant around the real images $\pi = p_r + \epsilon$, where $\epsilon \sim N_d(0, cI)$.

For relaxing the gradient direction, Zhou [86] et al. believe that restricting the global Lipschitz constant might be unnecessary. Therefore, only maximum gradient is necessary to be penalized:

$$\mathcal{L}_{GP} = \left(\max_{\hat{x} \sim \pi} \|\nabla D_{\theta}(\hat{x})\|_2 - 1 \right)^2, \quad (40)$$

where $\pi = t \cdot p_r + (1-t) \cdot p_g$; Furthermore, inspired by Virtual Adversarial Training (VAT) [95], Dávid et al. [87] propose a method, called Adversarial Lipschitz Regularization (ALR), which restricts the 1-Lipschitz continuity at $\pi = p_r \cup p_g$ with the direction of adversarial perturbation. The proposed ALP shows the SOTA performance in terms of Inception Score and Fréchet Inception Distance among non-progressive growing methods trained on CIFAR-10 dataset.

Different from the above methods penalizing the gradient in the Euclidean space, Adler et al. [88] extended the L_p ($p = 2$) space with gradient penalty to Banach space that contains the L_p space and Sobolev space. For the Banach space B , the Banach norm $\|\cdot\|_B$ can be defined as:

$$\|x^*\|_{B^*} = \sup_{x \in B} \frac{x^*(x)}{\|x\|_B}. \quad (41)$$

Thus, the gradient penalty of Banach wasserstein GAN can be expressed as:

$$\mathcal{L}_{GP} = \mathbb{E}_{\hat{x} \sim \pi} (\|\nabla D_{\theta}(\hat{x})\|_{B^*} - 1)^2, \quad (42)$$

where $\pi = t \cdot p_r + (1 - t) \cdot p_g$.

2) k -GP ($k \leq 1$): k -GP ($k \leq 1$) is first applied by Gulrajani et al. [49] during the training of GANs, named WGAN-LP. WGAN-LP also uses the 2-norm gradient penalty across the entire image domain, which can be formulated as:

$$\mathcal{L}_{GP} = \mathbb{E}_{\hat{x} \sim \pi} \left[(\max\{0, \|\nabla D_{\theta}(\hat{x})\|_2 - 1\})^2 \right], \quad (43)$$

where π is the distribution of entire image space approximated by the interpolation of real distribution (p_r) and generated distribution (p_g): $\pi = t \cdot p_r + (1 - t) \cdot p_g$ for $t \sim U[0, 1]$. Furthermore, Xu et al [89] show a more general dual form of the Wasserstein distance compared to KR duality (mentioned in section 2.3), named Sobolev duality, which relaxes the Lipschitz constraint but still maintains the favorable gradient property of the Wasserstein distance. They also show that the KR duality is a special case of the proposed Sobolev duality. Based on the Sobolev duality, the relaxed gradient penalty of the proposed SWGAN can be formulated as:

$$\mathcal{L}_{GP} = \mathbb{E}_{\hat{x} \sim \pi} \left[\left(\max\{0, \|\nabla D_{\theta}(\hat{x})\|^2 - 1\} \right)^2 \right], \quad (44)$$

where $\pi = t \cdot p_r + (1 - t) \cdot p_g$ for $t \sim U[0, 1]$. It is clear that both the WGAN-LP and the SWGAN have the same form of gradient penalty. Different relaxation methods yield the same form of regularization, which is exciting.

3) 0-GP: 0-GP is first implemented by Wu et al. [66], where Wasserstein divergence is introduced. According to [96], Wasserstein divergence can be solved by minimizing:

$$\mathcal{L}_{GP} = \mathbb{E}_{\hat{x} \sim \pi} \|\nabla D_{\theta}(\hat{x})\|^2, \quad (45)$$

where π is both the real distribution (p_r) and the generated distribution (p_g): $\pi = p_r \cup p_g$. Furthermore, Mescheder et al. [80] also demonstrate that the optimization of unregularized GAN is not always locally convergent and some simplified zero centered gradient penalty (zc-GP) technologies, implemented by minimizing Eq (45), can be used to achieve local convergence of GANs.

Besides, some other 0-GP methods [67], [90]–[92] are derived by different theoretical derivations. Specifically, Su et al. [67] propose a Quadratic Potential (QP) for GANs training, which can be formulated as:

$$\mathcal{L}_{GP} = \mathbb{E}_{x_r, x_g \sim \pi} \frac{(D_{\theta}(x_r) - D_{\theta}(x_g))^2}{\|x_r - x_g\|}, \quad (46)$$

where π is the joint distribution of the real and generated distributions: $\pi = p_r \cdot p_g$; Zhang et al. [90] combine a Total Variational (TV) regularizing term into the training of GANs, that is $|D_{\theta}(x_r) - D_{\theta}(x_g) - \delta|$. According to the [90], the TV term can be approximated by Eq (45), which is exhilarating; Zhou et al. [91] propose the Lipschitz GANs, with the maximum of the gradients penalty for guaranteeing the gradient informativeness:

$$\mathcal{L}_{GP} = \max_{\hat{x} \sim \pi} \|\nabla f(\hat{x})\|_2^2, \quad (47)$$

where $\pi = t \cdot p_r + (1 - t) \cdot p_g$; Thanh-Tung et al. [92] also propose the 0-GP with gradients penalty at $\pi = t \cdot p_r + (1 - t) \cdot p_g$:

$$\mathcal{L}_{GP} = \mathbb{E}_{\hat{x} \sim \pi} \|\nabla f(\hat{x})\|_2^2. \quad (48)$$

TABLE III: The experimental results of different Gradient penalty

Method	Inception Score	FID
WGAN-GP [31]	7.869	16.62
WGAN-LP [49]	7.98	15.85
WGAN-ALP [87]	8.247	14.19
WGAN-GP-Max [86]	7.956	18.43
WGAN-ZP-Max [91]	7.908	17.97
WGAN-ZP-Sample [80]	8.013	15.87
WGAN-ZP [92]	7.957	16.08

TABLE IV: The summary of the weight normalization and wight regularization

Method	Implementation	Motivation
Spectral normalization (SN) [46]	$W_{\sigma} = W / \ W\ _2$	$\ D\ _{Lip} \rightarrow 1$
F normalization [46]	$W_{\sigma} = W / \ W\ _F$	$\ D\ _{Lip} \leq 1$
Mixed normalization [99]	$W_{\sigma} = W / \sqrt{\ W\ _1 \ W\ _{\infty}}$	$\ D\ _{Lip} \leq 1$
Spectral increment normalization [100]	$W_{\sigma} = W / (\ W\ _2 + \nabla W / \ W\ _2)$	$\ D\ _{Lip} \rightarrow 1$
Off-Diagonal Orthogonal regularization (Off-Diagonal OR) [30]	$R_O(W) = \beta \ W^T W \odot (I - I)\ _F^2$	Smoothing G

In summary, gradient penalty technologies are widely used in the GANs training to achieve Lipschitz continuity of discriminator. As shown in TABLE II, too many similar techniques are proposed based on different theories and phenomena. But as far as we know, there is no fair and comprehensive work comparing the performance of these gradient penalty methods. To compare the performance of various methods intuitively, a comparative experiment on the CIFAR-10 dataset is conducted.

To compare the performance of various methods intuitively, a comparative experiment on the CIFAR10 dataset is conducted. The results of its Inception Score (IS) [97], [98] and FID [20] are shown in TABLE III. The results show that WGAN-ALP achieves a much better performance compared with WGAN-GP, while other methods based on gradient penalty do not bring much improvement. Among these methods, some [86], [91] even lead to the worse performance with the FID measurement, such as the penalty on maximum gradient. More precisely, limiting the Lipschitz constant in the direction of adversarial perturbation can achieve better results, and for the Lipschitz constant, it is better to limit it to zero instead of one.

B. Weight Normalization and Weight Regularization

1) *Weight Normalization*: Lipschitz continuity is important for GANs training. From Section 2.4, spectral norm of the weight and the Lipschitz constant express the same concept. To meet the Lipschitz continuity, in addition to the gradient penalty, weight normalization can also be used. Spectral normalization of the weight can limit the Lipschitz constant to 1. Certainly, upper bound of the spectral norm can be used to normalize the weights, achieving $k(k \leq 1)$ Lipschitz continuity. The following lemmas put forward some upper bounds of the spectral norm.

Lemma 3.1: If $\lambda_1 \leq \lambda_2 \leq \dots \leq \lambda_M$ are the eigenvalues of the $W^T W$, then the spectral norm $\|W\|_2 = \sqrt{\lambda_M}$; The Frobenius norm $\|W\|_F = \sqrt{\sum_{i=1}^M \lambda_i}$

Proof 3.1: See [101] and [46] \square

Lemma 3.2: For a $n \times m$ matrix, $\|W\|_1 = \max_j \sum_{i=1}^n |a_{i,j}|$,

$\|W\|_\infty = \max_i \sum_{j=1}^m |a_{i,j}|$, then $\|W\|_2 \leq \sqrt{\|W\|_1 \|W\|_\infty}$

Proof 3.2: See [101] \square

Lemma 3.3: For a $n \times m$ matrix, $\|W\|_F = \sqrt{\sum_{j=1}^m \sum_{i=1}^n |a_{i,j}|^2}$, then $\|W\|_2 \leq \|W\|_F$

Proof 3.3: See [101] \square

1-Lipschitz continuity can be expressed by the spectral normalization. Miyato et al. [46] control the Lipschitz constant through spectral normalization $W_\sigma = \frac{W}{\|W\|_2}$ of each layer for D, leading to a better result than WGAN-GP. Similarly, according to the optimal transport with regular term, Lipschitz constant of discriminator should be less than or equal to 1. Correspondingly, upper bound of the spectral norm can be utilized to normalize the weight ($\|W_\sigma\|_2 \leq 1$), achieving $k(k \leq 1)$ Lipschitz continuity. In terms of Lemma 3.2 and Lemma 3.3, $\sqrt{\|W\|_1 \|W\|_\infty}$ and Frobenius norm ($\|W\|_F$) are simple upper bound of the spectral norm ($\|W\|_2$) and can be used to normalize the weight. Specifically, Zhang et al. [99] use the $\sqrt{\|W\|_1 \|W\|_\infty}$, seeking for an approximation of the spectral norm that is easy to calculate. Miyato et al. [46] explain that the Frobenius norm is a restriction on all eigenvalues. It is different from the spectral norm, which only constrains the maximum eigenvalue. They only propose a conjecture that Frobenius normalization will affect the network's ability to express, but no experiments are reported to compare it with the spectral normalization. Liu et al. [100] find that the mode collapse is often accompanied by the collapse of the eigenvalue of the discriminator. Because the spectral normalization only limits the maximum eigenvalue, and the eigenvalue collapse means the remaining eigenvalues suddenly decreasing. Therefore, they adopt the following methods to prevent the collapse of the eigenvalues:

$$W_\sigma = \frac{W + \nabla W}{\|W\|_2} = \frac{W}{\|W\|_2} + \frac{\nabla W}{\|W\|_2}. \quad (49)$$

The results demonstrate that this simple method can effectively prevent mode collapses. Experiments are reported in this study, yet theoretical proofs are not absent. Therefore the relationship between the matrix eigenvalues and GAN performance is not clear.

Few researches focus on weight normalization, whose summary is demonstrated in TABLE IV. Among them, spectral normalization is widely applied in some SOTA methods, which is demonstrated in Section 7.

2) *Weight Regularization:* Compared with spectral normalization similar to 1-GP, spectral norm regularization is similar to the 0-GP. Therefore, Kurach et al. [51] use the $\mathcal{L}_R = \|W\|_2$ to regularize the loss function. Besides, Zhou et al. [102] also use the L_P -norm ($P = 1, F, \infty$) to regularize the discriminator. However, researchers are not involved in the related study of these methods as they lead to worse performance than spectral normalization.

In addition to the above methods being used to implement Lipschitz continuity for discriminators, Brock et al. [30] apply Off-Diagonal Orthogonal Regularization (Off-Diagonal OR) to the generator directly enforcing the orthogonality condition:

$$R_o(W) = \beta \|W^T W \odot (\mathbf{1} - I)\|_F^2, \quad (50)$$

where W is a weight matrix, β is a hyperparameter and $\mathbf{1}$ denotes a matrix with all elements set to 1. The Off-Diagonal OR makes G to be smooth, so that the full space of z will map to good output samples.

V. REGULARIZATION AND NORMALIZATION OF "MAKING SAMPLE REAL"

From the perspective of the "Making sample real", generator is counterfeiter designed to deceive the discriminator, while discriminator is police designed to distinguish between real and fake samples. The motivation of GANs is to train the generator based on the loss of the discriminator. Unlike the direct training objective of the classification task (Minimizing cross-entropy loss), the objective of GANs training is indirect. Hence, only one-dimensional output of the discriminator does not provide a complete representation on truth or false of samples. Some works have shown that the present discriminators contain some significant deficiencies in the frequency domain [27] and attribute domain [44], which are evidence of the lacking discrimination for discriminators. Excessive shortage of discrimination makes the generator lack incentives from the discriminator to learn useful information of the data. To alleviate this situation, many regularization methods and additional supervision tasks have been proposed in the community, and they can be divided into three categories: **data augmentation and preprocessing**, **consistency regularization**, and **self-supervision**.

A. Data Augmentation and Preprocessing

Data Augmentation has played an important role in deep learning algorithms. It can increase the diversity of the training data naturally, thus reduce the overfitting in many computer vision and graphics applications [103], [104]. Data augmentation adopts different data transformation technologies (T) to increase the number of training samples. According to the different forms, data transformations can be divided into two types. One type is spatial transformation of data, such as *zoomout*, *zoomin*, *translation*, *translationx*, *translationy*, *cutout* [105], *cutmix* [106]; The other is visual transformation, such as *brightness*, *redness*, *greenness*, *blueness*, *mixup* [107].

Similarly, the performance of GANs heavily deteriorates given a limited amount of training data [108]. However, recent works [47], [48], [109]–[111] observe that augmenting only real images (Only applying T to (i) in Figure 3), only generated images (Only applying T to (ii) in Figure 3), and only discriminator (Both applying T to (i) and (ii) in Figure 3) do not help with GANs training. Naturally, one problem needs to be considered: whether the overfitting exists in GANs' training? Some works [47], [110] demonstrate that, even big dataset and state of the art models, the training of GANs

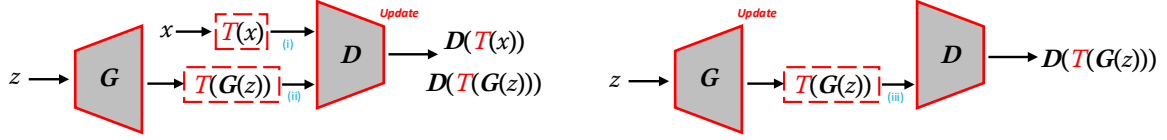


Fig. 3: Framework of data augmentation and preprocessing for updating D (left) and G (right). (Coming from [47])

still suffers from severe overfitting. And the less training data there is, the earlier this happens. Recently, some works [47], [109]–[111] on data augmentation for GANs training have been proposed simultaneously. They all argue that the classical data augmentation approach could mislead the generator to learn the distribution of the augmented data, which could be different from that of the original data. To deal with this problem, they augment both real and fake samples and let gradients propagate through the augmented samples to G (Applying T to (i), (ii), and (iii) in Figure 3). Through adding the data augmentation to all processes of GANs training, the performance of GANs has been significantly improved. However, which augmentation is most beneficial for GANs training? Figure 4 shows the FID comparisons (demonstrated on [109]) of BigGAN on CIFAR-10 dataset. For only data augmentation (represented by ‘vanilla_rf’), the operations in spatial augmentation such as *translation*, *zoomout*, and *zoomin*, are much more effective than the operations in visual augmentation, such as *brightness*, *colorness* (*redness* and *greenness*), and *mixup*. The result is that augmentations resulting in spatial changes improve the GANs performance more than those inducing mostly visual changes. It is easy to understand that generated images are significantly lacking in detail compared to the real images, and spatial augmentation improves the ability of the generator to fit detailed textures through spatial changes.

In addition to data augmentation, Li et al. [45] indicate that high-frequency components between real images and fake images are different, which is not conducive to the training of GANs. They propose two preprocessing methods eliminating high-frequency differences in GANs training: High-Frequency Confusion (HFC) and High-Frequency Filter (HFF). The proposed methods are applied in places (i), (ii), and (iii) in Figure 3 and improve the performance of GANs with a fraction of the cost.

In summary, both data augmentation and data preprocessing improve the performance of GANs with little cost. Data augmentation uses different transformations to improve discrimination and avoid overfitting. Among them, spatial augmentations achieve better performance than visual augmentations. More specifically, Zhao et al. [47] demonstrate that hybrid augmentation with *Color+Translation+Cutout* is especially effective, and which is widely used in other works [112], [113]. Besides, data preprocessing is also a remarkable method. We expect more work to be presented in this area.

B. Consistency Regularization

For semi-supervised or unsupervised learning, consistency regularization has been widely used in [114]–[117]. It is

motivated by the fact that models should produce consistent predictions given input and their semantics-preserving augmentations, such as image rotating, and adversarial attacks. As acknowledged, the supervision of GANs training is weak. To increase the discrimination of discriminator, some consistency regularization technologies have also been used. Due to different goals, we divide them into two parts: *image consistency* and *network consistency*. The overviews of them are demonstrated in Figure 5.

1) *Image Consistency*: The purpose of GANs is to generate fake images similar to real ones. In GANs, the discriminator is generally used to distinguish real images and generated images. However, outputs of the discriminator with only one dimension hardly portray the authenticity of the image completely. To improve the representation of the discriminator, some works extend the outputs of the discriminator, for example, relativistic discriminator [118], [119], distribution discriminator [120], and cascading rejection [121]. While some works reduce the training difficulty of discriminators by introducing prior information. Regularizing the distance between the generated and real images with different measurements, namely image consistency, is the focus of this paper. The overview of it is demonstrated in left part of Figure 5, where consistency regularization is used to update generator (G) and can be formulated as:

$$\mathcal{L}_C = \mathbb{E}_{x \sim p_r, z \sim p_z} C(H(x), H(G(z))), \quad (51)$$

where H is the feature mapping function and C is the consistency measurement function. Different image consistency regularization have different H and C . Specifically, Salimans et al. [97] recommend that the generator should be trained using a feature matching procedure. The objective is:

$$\mathcal{L}_C = \|\mathbb{E}_{x \sim p_r} f(x) - \mathbb{E}_{z \sim p_z} f(G(z))\|_2^2, \quad (52)$$

where $f(x)$ denotes the intermediate layer of the discriminator. Similarly, the intermediate layer of another pre-trained classification model is also alternative. The empirical results indicate that feature matching is indeed effective in situations where normal GAN becomes unstable. Unlike the above work only using mean feature matching to train generators, Mroueh et al. [122] propose McGAN, which trains both the generator and discriminator using the mean and covariance feature matching. The objective is:

$$\begin{aligned} \mathcal{L}_C &= \mathcal{L}_\mu + \mathcal{L}_\sigma \\ &= \|\mu(p_r) - \mu(G(p_z))\|_q + \|\sum(p_r) - \sum(p(G(z)))\|_k, \end{aligned} \quad (53)$$

where $\mu(p_r) = \mathbb{E}_{x \sim p_r} f(x)$ and $\sum(p_r) = \mathbb{E}_{x \sim p_r} f(x) \cdot f(x)^T$ represent the mean and the covariance of the feature layer

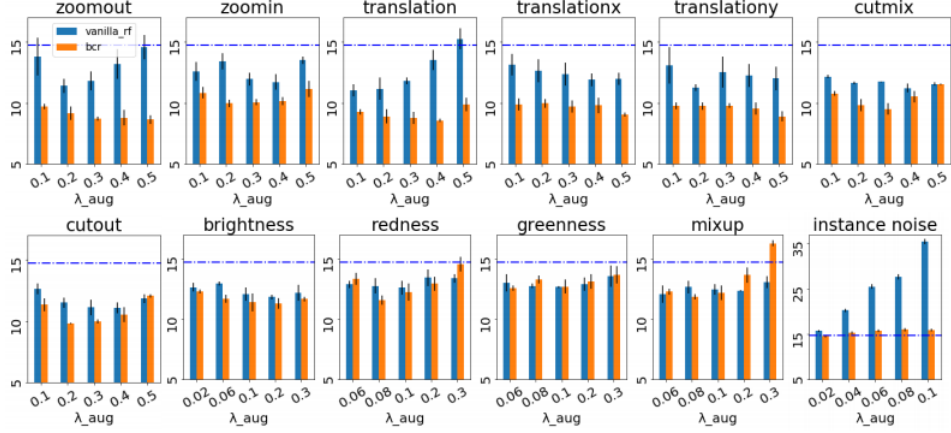


Fig. 4: FID mean and std of BigGAN on CIFAR-10. The blue dashed horizontal line shows the baseline FID=14.73 of BigGAN trained without augmentation. ‘vanilla_rf’ represents training vanilla BigGAN with both real and fake images augmented. ‘bcr’ corresponds to training BigGAN with bCR on augmented real and fake images. (Figure comes from [109])

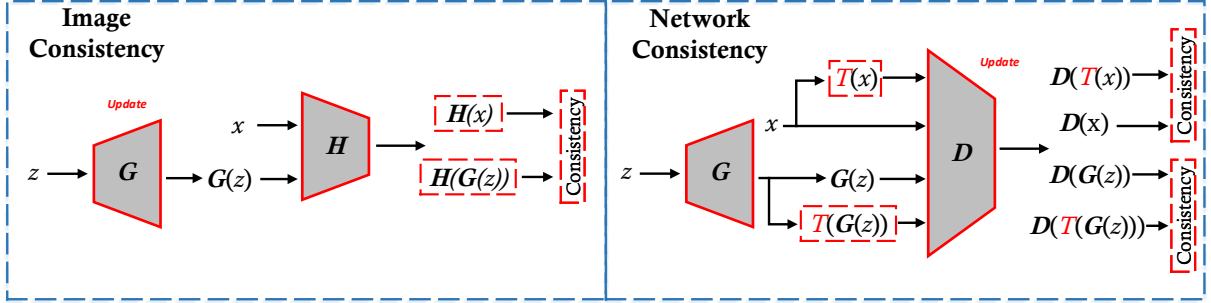


Fig. 5: Overview of consistency regularization, where image consistency regularization updates the G (left) and network consistency regularization updates the D (right). H is the feature mapping function and T is different data transformation technologies.

$f(x)$, respectively. Apart from statistical differences, some works [27], [123] focus on the difference in frequency domain between the generated and real image. Specifically, Durall et al. [123] find that the deep generative models based on up-convolution are failing to reproduce spectral distributions, which leads to considerable differences in the spectral distributions between real images and generated images. Thus, the spectral regularization has been proposed as follows:

$$\mathcal{L}_C = \frac{1}{M/2-1} \sum_{i=0}^{M/2-1} AI_i^{real} \cdot \log(AI_i^{fake}) + (1 - AI_i^{real}) \cdot \log(1 - AI_i^{fake}), \quad (54)$$

where M is the image size and AI is the spectral representation from the Fourier transform of the images. Corresponding to Eq (51), H and C are implemented with AI and cross-entropy, respectively.

Not the same as the above paradigm, some work [27] uses hard example mining to improve the discriminatory of the discriminator based on the difference between real and generated samples under different metrics. Although this

paradigm is different from the paradigm of image consistency regularization, they are both motivated by obtaining generated samples similar to real images under different distance measures, so we integrate them. Chen [27] et al. consider that both of these downsampling strategies: downsampling with anti-aliasing and downsampling without anti-aliasing, would lead to high frequencies missing in the discriminator. High frequencies missing will lead to high frequency deviation between real and generated images. To mitigate this issue, they propose SSD-GAN, which introduces an additional spectral classifier to detect frequency spectrum discrepancy between real and generated images and integrate it into the discriminator of GANs. The overall realness of sample x is represented as:

$$D^{ss}(x) = \lambda D(x) + (1 - \lambda)C(\phi(x)), \quad (55)$$

where the enhanced discriminator D^{ss} consists of two modules, a vanilla discriminator D that measures the spatial realness, and a spectral classifier C . λ is a hyperparameter that controls the relative importance of the spatial realness and the spectral realness. The adversarial loss of the framework can

be written as:

$$\mathcal{L}_D = \mathbb{E}_{x \sim p_{\text{data}}(x)} [\log D^{ss}(x)] + \mathbb{E}_{x \sim p_g(x)} [\log (1 - D^{ss}(x))] . \quad (56)$$

The summary of the image consistency regularization are demonstrated on Table V. In summary, image consistency considers that the real images and the generated images should be similar not only in the output of discriminator, but also in other perspectives, such as statistical information and frequency domain. More works will be presented with the analysis of the differences between real and generated images in different perspectives, which is interesting and meaningful.

2) *Network Consistency*: Network consistency regularization can be regarded as Lipschitz continuity on semantics-preserving transformation. Specifically, we hope discriminator is insensitive to semantics-preserving transformation, which drives the discriminator to pay more attention to the authenticity of the images. For example, in the image domain, the reality of images should not change if we flip the image horizontally or translate the image by a few pixels. To resolve this, Zhang et al. [48] propose the Consistency Regularization GAN (CR-GAN) that uses the consistency regularization on the discriminator during GANs training:

$$\mathcal{L}_C = \mathbb{E}_{x \sim p_r} \|D(x) - D(T(x))\|_2, \quad (57)$$

where $T(x)$ represents a transformation (shift, flip, cutout, etc.) of images. One key problem with the CR-GAN is that the discriminator might occur the 'mistakenly believe'. 'mistakenly believe' considers that the transformations are actual features of the target dataset, due to only applying these transformations on real images. This phenomenon is not easy to notice for certain types of transformations (e.g. image shifting and flipping). However, some types of transformations, such as cutout transformations, contain visual artifacts not belonging to real images, which effects greatly limits the choice of advanced transformations we could use. To address this issue, Zhao et al. [32] propose Balanced Consistency Regularization (bCR-GAN) that uses regulation with respect to both real and fake images and balances the training of discriminator between real images and fake images by λ_{real} and λ_{fake} :

$$\begin{aligned} \mathcal{L}_C = & \lambda_{real} \mathbb{E}_{x \sim p_r} \|D(x) - D(T(x))\|_2 \\ & + \lambda_{fake} \mathbb{E}_{z \sim p_z} \|D(G(z)) - D(T(G(z)))\|_2. \end{aligned} \quad (58)$$

The overview of bCR is demonstrated in right part of Figure 5.

Different from above two methods that only focus on consistency regularization with respect to transformations in image space, Zhao et al. [32] also propose Latent Consistency Regularization (zCR) that considers the consistency regularization on transformations in latent space. They expect that output of the discriminator ought not to change much with respect to the small enough perturbation Δz and modify the discriminator loss by enforcing:

$$\mathcal{L}_C^D = \lambda_{dis} \mathbb{E}_{z \sim p_z} \|D(G(z)) - D(G(T(z)))\|_2, \quad (59)$$

where $T(z)$ represents the added small perturbation noise. However, only this loss added onto the GAN loss, mode collapse can easily appear in the training of generators. To avoid this, an inverse gradient penalty (We will describe it in detail in section 6.2) is added to modify the loss function for generator. Hence, we modify the generator loss by enforcing:

$$\mathcal{L}_C^D = -\lambda_{gen} \mathbb{E}_{z \sim p_z} \|G(z) - G(T(z))\|_2. \quad (60)$$

Naturally, putting both bCR and zCR together, Improved Consistency Regularization (ICR) is also proposed by Zhao et al. [32]. In addition, there are some applications where cyclic consistency regularization [124] is used for unpaired image-to-image translation. The summary of network consistency regularization are demonstrated in TABLE V.

In summary, network consistency considers that the networks, especially the discriminator, should be insensitive to semantics-preserving transformation (T). The results in [48] demonstrate that random shift and flip is the best way to perform image transformation on the CIFAR-10 dataset. And the FID results with CR, bCR, zCR, and ICR (where transformation is flipping horizontally and shifting by multiple pixels) demonstrated on [32] are shown in Table VI. The results demonstrate that network consistency regularization can significantly improve the performance of GANs. However, which transformation is best for consistency regularization? Zhao et al [109] compare the effect of different data transformation technologies (mentioned in Section 5.1) on bCR. Figure 4 shows the FID results (demonstrated on [109]) of BigGAN adding bCR (represented by 'bcr') on CIFAR-10 dataset. From the results, the best BigGAN FID 8.65 is with transformation technology *translation* of strength $\lambda = 0.4$, outperforming the corresponding FID 10.54 reported in Zhao et al. [32]. Moreover, spatial transforms, which retain the major content while introducing spatial variances, can substantially improve GANs performance together with bCR. While visual transforms, which retain the spatial variances, can not further improve the performance of GANs compared with data augmentation only. Furthermore, bCR with stronger transformation (larger value of λ_{aug}) does not improve the performance of GANs, the optimal value of λ_{aug} is uncertain for different data transformation technologies.

C. Self-Supervision

Self-supervised learning aims to learn representations from the data itself without explicit manual supervision. Recently, some self-supervised works [117], [125], [126] provide competitive results on ImageNet classification and the representations learned from which transfer well to downstream tasks. Self-supervised learning can outperform its supervised pre-training counterpart in many tasks, such as detection and segmentation, sometimes surpassing it by large margins. This suggests that self-supervised learning can obtain more representational features and significantly improve the representation of networks. Based on this, self-supervised learning can be introduced into the training of GANs, and we divide them into two categories according to different self-supervision tasks: [predictive self-supervised learning](#) and [contrastive self-supervised learning](#).

TABLE V: The summary of the consistency regularization

Method	Consistency regularization term L_C
Mean regularization [97]	$\ \mathbb{E}_{x \sim p_r} f(x) - \mathbb{E}_{z \sim p_z} f(G(z))\ _q$
Mean and Covariance regularization [122]	$\ \mathbb{E}_{x \sim p_r} f(x) - \mathbb{E}_{z \sim p_z} f(G(z))\ _q + \ \mathbb{E}_{x \sim p_r} f(x) \cdot f(x)^T - \mathbb{E}_{z \sim p_z} f(G(z)) \cdot f(G(z))^T\ _k$
Spectral regularization [123]	$L_C = \frac{1}{M/2-1} \sum_{i=0}^{M/2-1} AI_i^{real} \cdot \log(AI_i^{fake}) + (1 - AI_i^{real}) \cdot \log(1 - AI_i^{fake})$
CR-GAN [48], [124]	$\mathbb{E}_{x \sim p_r} \ D(x) - D(T(x))\ _2$
bCR-GAN [32]	$\lambda_{real} \mathbb{E}_{x \sim p_r} \ D(x) - D(T(x))\ _2 + \lambda_{fake} \mathbb{E}_{z \sim p_z} \ D(G(z)) - D(T(G(z)))\ _2$
zCR-GAN [32]	$\lambda_{dis} \mathbb{E}_{z \sim p_z} \ D(G(z)) - D(G(T(z)))\ _2 - \lambda_{gen} \mathbb{E}_{z \sim p_z} \ G(z) - G(T(z))\ _2$

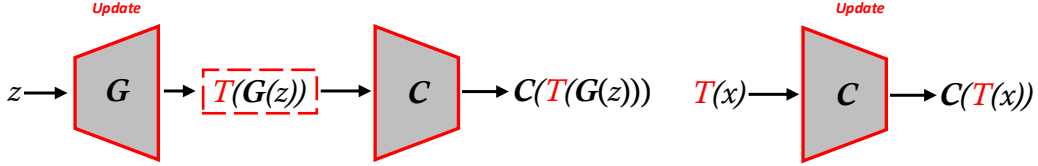


Fig. 6: Overview of the predict self supervised learning of GANs, where C performs the predict classification task and shares the weights with the discriminator except for the last layer, T is different data transformation technologies. Furthermore, the self-supervised task of generated images is used to update the generator (left) and the self-supervised task of real images is used to update the classification (right).

TABLE VI: FID scores for class conditional image generation of the network consistency regularization (Data come from [32])

Models	CIFAR-10	ImageNet
SNGAN	17.50	27.62
BigGAN	14.73	8.73
CR-BigGAN	11.48	6.66
bCR-BigGAN	10.54	6.24
zCR-BigGAN	10.19	5.87
ICR-BigGAN	9.21	5.38

1) *Predictive Self-Supervised Learning*: Predictive self-supervised learning is a popular method to improve the representation of neural networks by introducing additional supervised tasks, such as context prediction [127] and rotations prediction [128]–[131]. Predictive self-supervised learning is introduced into GANs by Chen et al. [26] to avoid discriminator forgetting. Discriminator forgetting means that the discriminator can not remember all tasks at the same time during the training process, for example, learning varying levels of detail, structure, and texture, which causes the discriminator to fail to get a comprehensive representation of the current images. "If the outcome is your focus, then it's easy to look for shortcuts. And ultimately shortcuts keep you from seeing the truth, it drains your spark for life. What matters most is your will to seek the truth despite the outcome."⁸. The same is true for GANs, which are only driven by the loss of discriminator, which is easy to distinguish between real

images and generated images through shortcuts, instead of the texture and structural features we need. Predictive self-supervised learning solves this problem by introducing new generalization tasks, which can also be considered to prevent overfitting. The overview of the predictive self-supervised learning of GANs are demonstrated on Figure 6. Depending on the data transformation function T , we can design different self-supervised tasks.

Chen et al. [26] used the predictive self-supervision in GANs training for the first time. They adopt the rotation prediction as the expanding task to prevent the discriminator from forgetting. Besides, plenty of other prediction tasks have also been proposed to improve the discrimination. Huang et al. [132] exploit the feature exchange to make the discriminator learn the proper feature structure of natural images. Baykal et al. [133] introduce a reshuffling task to randomly arrange the structural blocks of the images, thus helping the discriminator increase its expressive capacity for spatial structure and realistic appearance. Different from the methods described above for designing tasks at the image or feature level, Patel et al. [134] propose a self-supervised task with latent transformation detection, which identifies whether the latent transformation applied in the given pair is the same as that of the other pair. All above methods have designed different self-supervised tasks, and their loss functions can be formulated as:

$$\begin{aligned} \mathcal{L}_{D,C} &= -\lambda_r \mathbb{E}_{x \sim p_r^T} \mathbb{E}_{T_k \sim T} \log(C_k(x)) \quad \text{for } k = 1, \dots, K, \\ \mathcal{L}_G &= -\lambda_g \mathbb{E}_{x \sim p_g^T} \mathbb{E}_{T_k \sim T} \log(C_k(x)) \quad \text{for } k = 1, \dots, K, \end{aligned} \quad (61)$$

where T represents the different types of image transfer, such as rotation and reshuffling. Furthermore, T_k represents different forms of the transfer T , such as $0^\circ, 90^\circ, 180^\circ, 270^\circ$

⁸Come from "JoJo's Bizarre Adventure:Golden Wind" -Araki Hirohiko.

for rotation task, K is the number of transformed forms, C_k is the k -th output of the classifier C that shares parameters with discriminator except for two different heads, P_r^T and P_g^T are the mixture distributions of real and generated images, respectively. For rotation conversion task [26], $K = 4$, and the classifier C predicts the rotation angle; For feature exchange task [132], $K = 2$, and the classifier C predicts whether the swap has occurred; For block reshuffling task [133], the image is divided into 9 blocks and the number of the permutations is $9!$, which is unnecessarily huge. Thirty different permutations are selected in terms of the Hamming distances between the permutations in [135]. As a result, K is set to 30, and classifier C predicts the Hamming distances of different permutations; For the latent transformation task, $K = 2$, and the classifier C predicts whether the transformations parameterized by the same ϵ or different.

The above methods design different kinds of self-supervised prediction tasks and participate in the training of the discriminator or generator, independently, which have “loophole” that, during generator learning, G could exploit to minimize \mathcal{L}_G without truly learning the data distribution. To address this issue, Ngoc-TrungTran et al. [136] introduce true or false judgment along with self-supervised prediction. The number of classification is $K + 1$, while the loss function can be expressed as:

$$\begin{aligned} \mathcal{L}_{D,C} = & -\lambda_r \left(\mathbb{E}_{x \sim p_r^T} \mathbb{E}_{T_k \sim T} \log(C_k(x)) + \mathbb{E}_{x \sim p_r^T} \mathbb{E}_{T_{K+1} \sim T} \log(C_{K+1}(x)) \right) \\ & \text{for } k = 1, \dots, K, \\ \mathcal{L}_G = & -\lambda_g \left(\mathbb{E}_{x \sim p_g^T} \mathbb{E}_{T_k \sim T} \log(C_k(x)) - \mathbb{E}_{x \sim p_g^T} \mathbb{E}_{T_{K+1} \sim T} \log(C_{K+1}(x)) \right) \\ & \text{for } k = 1, \dots, K, \end{aligned} \quad (62)$$

where C_k is a classifier that predicts the rotation angles and C_{K+1} is a classifier that predicts the truth of the images. The new self-supervised rotation-based GANs use the multi-class minimax game to avoid the mode collapse, which is better than the original predictive self-supervised paradigm.

In summary, predictive self-supervised learning improves the discrimination by designing different self-supervised prediction tasks, among them, rotation prediction [26] is widely used ([47], [109]) for its simplicity and practicality. The summary is illustrated in TABLE VII.

2) *Contrastive Self-Supervised Learning*: Contrastive self-supervised Learning [117], [125], [126], as the name implies, learn representations by contrasting positive and negative examples. They led to great empirical success in computer vision tasks with unsupervised contrastive pre-training. More and more works demonstrate that self-supervised learning can outperform its supervised pre-training counterpart in many tasks, which indicates contrastive self-supervised learning can lead to more expressive features. Consider two views ($v^{(1)}$ and $v^{(2)}$), contrastive self-supervised learning aims to identify whether two views are dependent or not. More specifically, Oord et al. [138] propose to minimize InfoNCE loss, which

turns out to maximize a lower bound of mutual information. the InfoNCE loss is defined by:

$$L_{\text{NCE}}(v_i^{(1)}; v_i^{(2)}, s) := -\log \frac{\exp(s(v_i^{(1)}, v_i^{(2)}))}{\sum_{j=1}^K \exp(s(v_i^{(1)}, v_j^{(2)}))}, \quad (63)$$

where $s(\cdot)$ is the score function that measure the similarity, positive pairs ($v_i^{(1)}$ and $v_i^{(2)}$) are different views of the same sample, and negative pairs ($v_i^{(1)}$ and $v_j^{(2)}$, ($i \neq j$)) are different views of different samples. InfoNCE loss is the cornerstone of contrastive self-supervised learning and its overview is demonstrated on Figure 7.

Many advanced self-supervised methods are implemented by modifying the views of images $v^{(1)}$, $v^{(2)}$ and score function $s(\cdot)$. Specifically, Deep InfoMAX [139] maximizes the mutual information between local and global features, that is, image x passes through the encoder $E_\psi = f_\psi \circ C_\psi$, producing local feature map $C_\psi(x)$ and global feature vector $E_\psi(x)$. To maximize the lower bound of the InfoMax: $\mathcal{I}(C_\psi(x), E_\psi(x))$, the theoretical InfoMAX loss has been defined as:

$$\begin{aligned} L_{\text{InfoMAX}}(X) = & -\mathbb{E}_{x \in X} \mathbb{E}_{i \in \mathcal{A}} \left[\log \frac{\exp(g_{\theta, \omega}(C_\psi^{(i)}(x), E_\psi(x)))}{\sum_{(x', i) \in X \times \mathcal{A}} \exp(g_{\theta, \omega}(C_\psi^{(i)}(x'), E_\psi(x')))} \right], \\ & g_{\theta, \omega}(C_\psi^{(i)}(x), E_\psi(x)) = \phi_\theta(C_\psi^{(i)}(x))^T \phi_\omega(E_\psi(x)), \end{aligned} \quad (64)$$

where $X = \{x_1, \dots, x_N\}$ is a set of random images and $\mathcal{A} = \{0, 1, \dots, M^2 - 1\}$ represents indices of a $M \times M$ spatial sized local feature map. Based on this, positive sample pairs are $C_\psi^{(i)}(x)$ and $E_\psi(x)$, and negative sample pairs are $C_\psi^{(i)}(x')$ and $E_\psi(x)$, where x' is a different image from x . SimCLR [117] is another popular contrast learning framework, which applies two independent transformations, namely t_1 and t_2 , to obtain the different views $v^{(1)}, v^{(2)} = t_1(x), t_2(x)$. Then the loss function of SimCLR is defined as:

$$L_{\text{SimCLR}}(v^{(1)}, v^{(2)}) = \frac{1}{N} \sum_{i=1}^N \left(L_{\text{NCE}}(v_i^{(1)}; [v_i^{(2)}; v_{-i}^{(1)}], s_{\text{SimCLR}}) \right), \quad (65)$$

where $v_{-i} := v \setminus \{v_i\}$ and s_{SimCLR} is defined as:

$$s_{\text{SimCLR}}(v^{(1)}, v^{(2)}; f, h) = \frac{h(f(v^{(1)})) \cdot h(f(v^{(2)}))}{\tau \cdot \|h(f(v^{(1)}))\|_2 \|h(f(v^{(2)}))\|_2}. \quad (66)$$

As shown in Figure 7, SimCLR defines more negative pairs to improve the sample utilization compared to InfoNCE.

The self-supervised methods mentioned above are also widely applied to the training of GANs. Inspired by Deep InfoMax [139], Lee et al. [137] propose InfoMax-GAN maximizing the mutual information between local and global features of real and fake images. The regularization of discriminator can be expressed as:

$$\mathcal{L}_{\text{InfoMax-GAN}} = \lambda_d \{L_{\text{InfoMAX}}(x_r) + L_{\text{InfoMAX}}(x_f)\}. \quad (67)$$

where x_r and x_f represent sets of real and fake images, respectively.

TABLE VII: The summary of the Self-supervision

Method	Description	Types
Rotation Prediction [26], [136]	Predicting the angle of rotation ($0^\circ, 90^\circ, 180^\circ, 270^\circ$)	Predictive self-supervised
Feature Exchange Detection [132]	Predicting if some exchanges have occurred at the feature level (yes or not)	Predictive self-supervised
Block Reshuffling Prediction [133]	Predicting the Hamming distances of different reshuffling in image level (Total 30 categories)	Predictive self-supervised
Latent Transformation Detection [134]	Predicting if some exchanges have occurred at the latent space level (yes or not)	Predictive self-supervised
InfoMax-GAN [137]	Positive pairs: Global and local features of an image (both real and fake images) Negative pairs: Global and local features of different images (both real fake images)	Contrastive self-supervised
Cntr-GAN [109]	Positive pairs: Two different data transformations of the same image (both real and fake images). Negative pairs: Otherwise	Contrastive self-supervised
ContraD [112]	Positive pairs: Two different data transformations of the same image (real images only) + Two fake images Negative pairs: Otherwise	Contrastive self-supervised

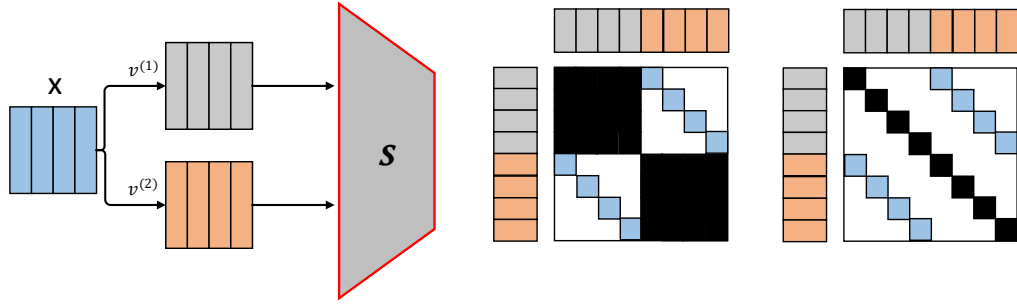


Fig. 7: Overview of the contrastive self supervised learning, where x is real or fake images, $v^{(1)}$ and $v^{(2)}$ are different views of the image x , s is the score function (Usually discriminator in GANs) that measures the similarity, the square on the middle part is the label of InfoNCE (blue, white, and black squares are labels with 1, 0, and undefined respectively.), and the square on the right part is the label of SimCLR. Obviously, SimCLR defines more negative pairs to improve the sample utilization.

Inspired by SimCLR [117], some methods [109], [112] introduce different data transformation technologies to create positive and negative pairs during GANs training. Zhao et al [109] propose Cntr-GAN, where SimCLR loss is used to regularize the discriminator on two random augmented copies of both real and fake images. The regularization of discriminator for transformation T is:

$$\mathcal{L}_{\text{Cntr-GAN}} = \lambda_d \{L_{\text{SimCLR}}(x_r, T(x_r)) + L_{\text{SimCLR}}(x_f, T(x_f))\}. \quad (68)$$

They also compare the effect of different data transformation technologies (mentioned in Section 5.1) on Cntr-GAN. Figure 8 shows the FID results (demonstrated on [109]) of BigGAN adding SimCLR loss on CIFAR-10 dataset. The results illustrate that spatial transformations still work better than visual transformations and the best FID of 11.87 is achieved by applying adjusted SimCLR transformations with the cropping/resizing strength of 0.3. Although this simply regularizing auxiliary SimCLR loss improves GAN training, but could not outperform existing methods based on simple data augmentations, *e.g.*, bCR (demonstrated in Figure 4).

To improve the efficiency of contrastive learning, Jeong et al. [112] propose Contrastive Discriminator (ContraD), a way of training discriminators of GANs using improved SimCLR. Different from Cntr-GAN with SimCLR loss on both real and generated images, ContraD uses the SimCLR

loss on the real images and the supervised contrastive loss on the generated images. Supervised contrastive loss adopts the contrastive between real and generated images, which is needed as a GAN discriminator. More concretely, for two views $v^{(1)}, v^{(2)} = t_1(x), t_2(x)$ with $t_1, t_2 \sim T$, the loss of real images are:

$$L_{\text{con}}^+(D, h_r) = L_{\text{SimCLR}}(v_r^{(1)}, v_r^{(2)}; D, h_r), \quad (69)$$

where h_r is a projection head for this loss. However, the loss for generated images, an extended version of contrastive loss to support supervised learning by allowing more than one view to be positive. More concretely, they assume all the views from fake samples have the same label against those from real samples. Formally, for each $v_i^{(1)}$, the positive views are represented by $V_{i+}^{(2)}$ that is a subset of $v^{(2)}$. Then the supervised contrastive loss is defined by:

$$L_{\text{SupCon}}(v_i^{(1)}, v^{(2)}, V_{i+}^{(2)}) = -\frac{1}{|V_{i+}^{(2)}|} \sum_{v_{i+}^{(2)} \in V_{i+}^{(2)}} \log \frac{\exp(s_{\text{SimCLR}}(v_i^{(1)}, v_{i+}^{(2)}))}{\sum_j \exp(s_{\text{SimCLR}}(v_i^{(1)}, v_j^{(2)}))}. \quad (70)$$

Using the notation, the ContraD loss for fake samples are:

$$L_{\text{con}}^-(D, h_f) = \frac{1}{N} \sum_{i=1}^N L_{\text{SupCon}} \left(v_{f,i}, \left[v_{f,-i}; v_r^{(1)}; v_r^{(2)} \right], \left[v_{f,-i} \right]; D, h_f \right), \quad (71)$$

where $v_f = t_3(G(z))$ is a random view of fake samples ($t_3 \sim T$), and $v_{-i} = v \setminus \{v_i\}$ is subset of v that does not contain v_i . Remark that they also use an independent projection header h_f in this loss instead of h_r in $L_{\text{con}}^+(D, h_r)$.

To sum up, ContraD learns its contrastive representation by minimizing the following regularization loss:

$$L_{\text{con}}(D, h_r, h_f) = L_{\text{con}}^+(D, h_r) + \lambda_{\text{con}} L_{\text{con}}^-(D, h_f). \quad (72)$$

The experimental results show that ContraD consistently improves the performance of GANs compared to other methods, such as Cntr-GAN, DiffAug, bCR, and CR. However, ContraD with different data transformations is not discussed further.

In summary, contrastive self-supervised learning designs different positive and negative pairs and maximizes the mutual information of positive pairs according to the InfoNCE loss. Different from classification and segmentation tasks, two types of samples (real and fake images) exist for generating adversarial networks, which adds more possibilities to the definition of positive and negative pairs. In the future, score-based contrastive learning may be proposed during the training of GANs. The summary of contrastive self-supervised regularization technologies of GANs are illustrated in TABLE VII.

VI. REGULARIZATION AND NORMALIZATION OF "OTHER METHODS"

In addition to the three groups mentioned above, this section summarizes and discusses the remaining regularization and normalization techniques, namely, layer normalization and inverse gradient penalty. Specifically, **layer normalization** consists of unconditional-based layer normalization and conditional-based layer normalization, the former inspired by supervised learning is used to accelerate training, but its impact on the GANs is small and sometimes affects the performance, while the latter is used in the conditional generation and significantly improves the performance of conditional generation; Furthermore, **inverse gradient penalty** mitigates mode collapse by maximizing the Lipschitz constant of the generator.

A. Layer Normalization

Data in machine learning is expected to be independent and identically distributed (*i.i.d.*). However, in terms of deep learning, because of the Internal Covariate Shift (ICS) [40], inputs of each neuron can not satisfy the *i.i.d.*, which makes the training of the deep neural networks hard and unstable. Layer normalization⁹ has been proposed to avoid such problems. It is a simple approximation of the whitening which can resolve the ICS theoretically. The general form of the layer normalization

is (The difference between the normalization methods lies in the choice of h and the calculation of $\mathbb{E}[h]$ and $\text{var}[h]$):

$$h_N = \frac{x - \mathbb{E}[h]}{\sqrt{\text{var}[h] + \epsilon}} \cdot \gamma + \beta. \quad (73)$$

For GANs, the layer normalization can be divided into two parts: **unconditional-based layer normalization** and **conditional-based layer normalization**. Unconditional-based layer normalizations are used for unconditional generation similar to the other deep neural networks. On the other hand, conditional-based layer normalizations are used for the generator of the conditional generation, where the shift and scale parameters (γ, β) depend on the condition information. The form can be defined as:

$$h_N = \frac{x - \mathbb{E}[h]}{\sqrt{\text{var}[h] + \epsilon}} \cdot \gamma(c) + \beta(c). \quad (74)$$

1) Unconditional-based layer Normalization:

Unconditional-based layer normalization is used for both the generator and discriminator, whose motivation is the same as in other deep neural networks. Ioffe et al. [40] proposed the first normalization for neural networks, namely, Batch Normalization (BN). Batch normalization adopts the data of the mini-batch to compute the mean and variance, making the data distribution of each mini-batch approximately the same. Miyato et al. [46] used the BN in GANs. BN normalizes at the mini-batch level, which destroys the difference between pixels during the generation on account of image generation being a pixel-level task. Different from the BN normalizing the same channel with different images, Layer Normalization⁹ (LN) [41] normalizes different channels of a single image that also destroys the diversity between channels for the pixel-by-pixel generative model [46]. Instance Normalization (IN) [140] has also been proposed for style transformation that is adopted for a single channel of a single image. Moreover, Group Normalization (GN) [141] is between LN and IN, which first divides the channel into many groups, and then normalizes different groups of a single image. Comparing with the way that BN, LN, IN, and GN normalize the input of neural networks, Weight Normalization (WN) [142] normalizes the weight matrix of neural networks. Similarly, Miyato et al. [46] used this normalization in GANs.

In summary, unconditional-based layer normalization in GANs is the same as other neural networks. The related summaries are shown in TABLE IX. However, as far as we know, there is no work to compare the performance of these methods fairly, so we demonstrate the FID results for different normalization methods on CIFAR-10 and CIFAR-100 datasets in Figure VIII. Among them, LN and GN obtained better performance than the most popular normalization method: Spectral normalization (mentioned in Section 4.2). And other methods significantly affect the stability of GANs training.

2) *Conditional-based layer Normalization:* Conditional-based layer normalization is only used for the generator of the conditional generation. It aims to introduce conditional information to each layer of the generator, which helps to improve the quality of the generated images. $\gamma(c)$ and $\beta(c)$ in Eq (44) are calculated with different features or class labels as

⁹ layer normalization is different from the Layer Normalization (LN), where layer normalization is a general term for a class of methods such as BN, LN.

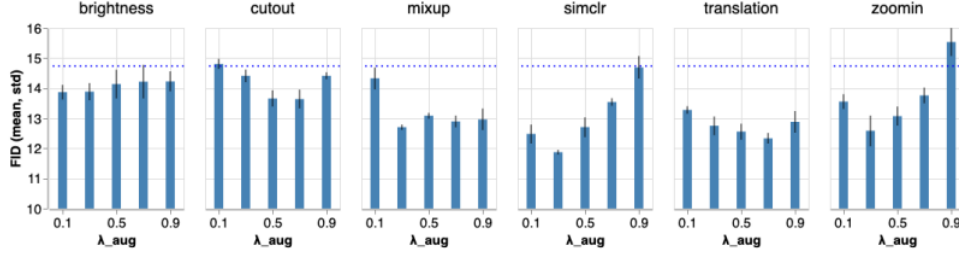


Fig. 8: BigGAN regularized by SimCLR loss with different image augmentations. The blue dashed horizontal line shows the baseline FID=14.73 of BigGAN trained without augmentation. Here they adjust the strength of cropping-resizing in the default simclr. Cntr-GAN consistently outperforms vanilla GAN with preference on spatial augmentations. (Figure comes from [109])

TABLE VIII: FID results for different normalization methods on CIFAR-10 and CIFAR-100 datasets. (The structure is the same as SNGAN except that the discriminator uses different normalization methods)

methods	CIFAR-10	CIFAR-100
None	40.91	45.44
BN	37.63	44.45
LN	19.21	21.15
IN	34.14	43.64
GN	19.31	20.80
WN	24.28	29.96
SN	19.75	22.89

input to the neural network in different methods. Miyato et al. [143] and Zhang et al. [144] used the Conditional Batch Normalization (CBN) to encode class labels, thereby improving the quality of conditional generation. Huang et al. [145] and Karras et al. [146] used the Adaptive Instance Normalization (AdaIN) with target images to improve the accuracy of style transfer. Park et al. [147] used the Spatially-Adaptive (de) Normalization (SPADE) with semantic segmentation image to incorporate semantic information into all layers. Wang et al. [148] used the Attentive Normalization (AN) to model long-range dependent attention, which is similar to self-attention GAN [144].

In summary, the main difference between these conditional-based normalizations is the content of conditional inputs (c in Eq (45)). As the information of inputs is gradually enriched, the performance of conditional generation is gradually improved. The related summaries are shown in TABLE IX.

B. Inverse Gradient Penalty

Mode collapse is a common phenomenon in GANs' training. Specifically, little changing of the generated space $G(z)$ along with the change in given latent variable z . Geometrically, the phenomenon means that all the tangent vectors of the manifold are no longer independent of each other - some tangent vectors either disappear or become linearly correlated

with each other. Intuitively, we can solve this problem by maximizing the Lipschitz constant of the generator, which is opposite of the gradient penalty of the discriminator described in the previous section. Based on this, inverse gradient penalty of the generator has been proposed. Concretely, under the little perturbation of the latent space, the generator needs to produce different images. Yang et al. [150] use it in conditional generation, especially for tasks that are rich in conditional information, such as inpainting and super-resolution.

$$\max_G \mathcal{L}_z(G) = \max_{z_1, z_2} \mathbb{E}_{z_1, z_2} \left[\min \left(\frac{\|G(y, z_1) - G(y, z_2)\|}{\|z_1 - z_2\|}, \tau \right) \right], \quad (75)$$

where y is the class label and τ is the bound to ensure numerical stability. Unlike the intuition-based work described above, Odena et al. [151] demonstrate that the decreasing of singular value in the Jacobian matrix of the generator is the main reason for the mode collapse during GANs training. Furthermore, the singular value can be approximated by the gradient, so Jacobian clamping is used to limit singular values to $[\lambda_{min}, \lambda_{max}]$. The loss can be expressed as:

$$\min_G \mathcal{L}_z(G) = (\max(Q, \lambda_{max}) - \lambda_{max})^2 + (\min(Q, \lambda_{min}) - \lambda_{min})^2, \quad (76)$$

where $Q = \|G(z) - G(z')\|/\|z - z'\|$.

In summary, the above two methods [150], [151] are similar and they can all mitigate the model collapse of generator to some extent. The key point is to improve the sensitivity of the generator to latent space.

VII. REGULARIZATION AND NORMALIZATION IN SOTA GANS

In this section, we investigate the regularization and normalization technologies that have been frequently employed in SOTA and popular GANs. We select five methods and they can be categorized into two classes according to different tasks: Unconditional Generation and Conditional Generation. The selected methods and analysis are shown in Table X. Specifically, PGGAN [29] is the most popular GAN model in recent years, which grows the size of both the generator and discriminator progressively. PGGAN empowers high-resolution image generation. Since PGGAN was proposed

TABLE IX: The summary of the layer normalization

Method	Reference	Classification	Inputs of $\gamma(c)$ and $\beta(c)$
Batch Normalization (BN)	2018 [46], [149]	unconditional-based	-
Layer Normalization (LN)	2018 [46]	unconditional-based	-
Instance Normalization (IN)	2018 [46]	unconditional-based	-
Group Normalization (GN)	2018 [141]	unconditional-based	-
Weight Normalization (WN)	2018 [46], [149]	unconditional-based	-
Conditional Batch Normalization (CBN)	2018 [143], [144]	conditional-based	class label
Adaptive Instance Normalization (AdaIN)	2017 [145], 2019 [146]	conditional-based	target images
Spatially-adaptive (de) Normalization (SPADE)	2019 [147]	conditional-based	semantic segmentation map
Attentive Normalization (AN)	2020 [148]	conditional-based	self

in 2017, only some simple regularization techniques were applied: WGAN-GP [31], BN [46], and LN [46]; AutoGAN [152] is the first study on introducing the Neural architecture search (NAS) to GANs. It defines the search space for the generator architecture and adopts Inception score as the reward to discover the best architecture. The discovered generator does not have any normalization, so AutoGAN only comprises SN [46]; BigGAN [30] is a popular conditional generative adversarial networks, which uses many regularization and normalization technologies, such as zc-GP [80], SN [46], Off-Diagonal OR [30], and CBN [143]; DiffAugment-CR-BigGAN [47] applies some latest regularization techniques to BigGAN and achieves better performance. Apart from the regularization and normalization techniques applied to BigGAN, CR [48] and data augmentation with *Translation + Cutout* are applied in it; Similarly, DiffAugment-StyleGAN2 [47] adds data augmentation with *Color + Cutout* to StyleGAN2 [153], where StyleGAN2 is also a popular conditional GANs. StyleGAN2 produces photorealistic images with large varieties and is widely used in image conditional generation tasks, such as Image Completion [154], Image-to-Image Translation [155]. Apart from the zc-GP and IN, path length regularization is also used in StyleGAN2.

In summary, too many regularization and normalization technologies have been used in SOTA GANs. Among them, zc-GP and SN are widely used. Furthermore, CR and Data augmentation are used to further improve the performance of GANs. They are orthogonal to and can be combined with other methods.

VIII. SUMMARY AND OUTLOOK

A. Summary

Recently, GANs have achieved remarkable results in generation tasks and have been widely used in many computer vision tasks, such as image inpainting, style transfer, text-to-image translations, and attribute editing. However, due to the overconfident assumptions, the training faces too many challenges, such as non-convergence, mode collapse, gradient vanishing, and overfitting. To mitigate these problems, many solutions focus on designing new architectures, new loss functions, new optimization methods, and regularization and normalization technologies.

In this paper, we understand the GANs training from three perspectives and propose a new taxonomy, denoted as "**Training dynamic**", "**Fitting distribution**", "**Making sample real**", and "**Other methods**", to survey the different regularization and normalization technologies during GANs training. Our work provides a systematic and comprehensive analysis of the reviewed methods to serve researchers of the community. In addition, we also demonstrate the motivation and purpose of different methods and compare the performance of some popular methods in a fair and quantitative way, which suggests a guideline when readers are selecting their research topics or developing their approaches.

B. Outlook

In the review of regularization and normalization of GANs, the following questions and thoughts are proposed based on different perspectives of GANs training:

- 1) What is a good distance metric, and what divergence should be used in GANs training? The priority in the training process of GANs is to find a suitable divergence to measure the distance between the generated distribution and the true distribution. Wasserstein divergence is important for the training of GANs. However, it's uncertain whether the next proposed divergence performs better.
- 2) What is the main difference between real images and generated images? During the training of unconstrained and unprioritized GANs, if we can quantitatively represent the difference between real images and generated images from different perspectives, the efficient regularization methods can be designed based on this.
- 3) How to avoid real images forgetting¹⁰? As acknowledged, real images do not directly participate in the training of the generator, thus the discriminator needs to remember the characteristics of the real images to optimize the generator indirectly. We call this the real images forgetting. We conjecture that real images forgetting may exist, and which may increase the difficulty of GANs training. Some works can be used to prove this hypothesis and propose effective solutions.

¹⁰Real images forgetting is caused by not introducing real images while training the generator, which is different from discriminator forgetting.

TABLE X: The survey of the Regularization and Normalization technologies used in SOTA GANs

Method	Task	Gradient Penalty	Weight normalization and regularization	Jacobian Regularization	Data augmentation and preprocessing	Consistency regularization	Self supervision	Layer normalization	Inverse gradient penalty
PGGAN (2017 [29])	Unconditional Generation	WGAN-GP	None	None	None	None	None	BN: G.LN: D	None
BigGAN (2018 [30])	Conditional Generation	zc-GP	SN: G, D Off-Diagonal OR	None	None	None	None	CBN	None
AutoGAN (2019 [152])	Unconditional Generation	None	SN-D	None	None	None	None	None	None
DiffAugment-CR-BigGAN (2020 [47])	Conditional Generation	zc-GP	SN: G, D Off-Diagonal OR	None	Translation Cutout	CR	None	CBN	None
DiffAugment-StyleGAN2 (2020 [47])	Conditional Generation	zc-GP	None	None	Color Cutout	None	None	IN	None

- 4) Recent works show that discriminator suffers from overfitting and discriminator forgetting. It is a common problem of neural networks, which is caused by the shortcut of the loss driven method. Some new methods, such as contrastive learning, representation learning, can be proposed to improve the generalization of the discriminator.

ACKNOWLEDGMENT

The work is partially supported by the National Natural Science Foundation of China under grand No.U19B2044, No.61836011 and No.91746209.

REFERENCES

- [1] I. Goodfellow, J. Pouget-Abadie, M. Mirza, B. Xu, D. Warde-Farley, S. Ozair, A. Courville, and Y. Bengio, "Generative adversarial nets," in *Advances in Neural Information Processing Systems*, 2014, pp. 2672–2680.
- [2] J. Yu, Z. Lin, J. Yang, X. Shen, X. Lu, and T. S. Huang, "Generative image inpainting with contextual attention," in *Proceedings of the IEEE Conference on Computer Vision and Pattern Recognition*, 2018, pp. 5505–5514.
- [3] U. Demir and G. Unal, "Patch-based image inpainting with generative adversarial networks," *arXiv preprint arXiv:1803.07422*, 2018.
- [4] K. Javed, N. U. Din, S. Bae, and J. Yi, "Image unmosaicing without location information using stacked gan," *IET Computer Vision*, vol. 13, no. 6, pp. 588–594, 2019.
- [5] A. Gonzalez-Garcia, J. Van De Weijer, and Y. Bengio, "Image-to-image translation for cross-domain disentanglement," in *Advances in Neural Information Processing Systems*, 2018, pp. 1287–1298.
- [6] A. Royer, K. Bousmalis, S. Gouws, F. Bertsch, I. Mosseri, F. Cole, and K. Murphy, "Xgan: Unsupervised image-to-image translation for many-to-many mappings," in *Domain Adaptation for Visual Understanding*. Springer, 2020, pp. 33–49.
- [7] H.-Y. Lee, H.-Y. Tseng, Q. Mao, J.-B. Huang, Y.-D. Lu, M. Singh, and M.-H. Yang, "Drit++: Diverse image-to-image translation via disentangled representations," *International Journal of Computer Vision*, pp. 1–16, 2020.
- [8] Y. Choi, Y. Uh, J. Yoo, and J.-W. Ha, "Stargan v2: Diverse image synthesis for multiple domains," in *Proceedings of the IEEE/CVF Conference on Computer Vision and Pattern Recognition*, 2020, pp. 8188–8197.
- [9] H. Zhang, T. Xu, H. Li, S. Zhang, X. Wang, X. Huang, and D. N. Metaxas, "Stackgan: Text to photo-realistic image synthesis with stacked generative adversarial networks," in *Proceedings of the IEEE International Conference on Computer Vision*, 2017, pp. 5907–5915.
- [10] T. Xu, P. Zhang, Q. Huang, H. Zhang, Z. Gan, X. Huang, and X. He, "Attngan: Fine-grained text to image generation with attentional generative adversarial networks," in *Proceedings of the IEEE Conference on Computer Vision and Pattern Recognition*, 2018, pp. 1316–1324.
- [11] T. Qiao, J. Zhang, D. Xu, and D. Tao, "Mirrorgan: Learning text-to-image generation by redescription," in *Proceedings of the IEEE Conference on Computer Vision and Pattern Recognition*, 2019, pp. 1505–1514.
- [12] Y. Shen, J. Gu, X. Tang, and B. Zhou, "Interpreting the latent space of gans for semantic face editing," in *Proceedings of the IEEE/CVF Conference on Computer Vision and Pattern Recognition*, 2020, pp. 9243–9252.
- [13] Y. Choi, M. Choi, M. Kim, J.-W. Ha, S. Kim, and J. Choo, "Stargan: Unified generative adversarial networks for multi-domain image-to-image translation," in *Proceedings of the IEEE conference on computer vision and pattern recognition*, 2018, pp. 8789–8797.
- [14] Z. He, W. Zuo, M. Kan, S. Shan, and X. Chen, "Attgan: Facial attribute editing by only changing what you want," *IEEE Transactions on Image Processing*, vol. 28, no. 11, pp. 5464–5478, 2019.
- [15] R. Tao, Z. Li, R. Tao, and B. Li, "Resattr-gan: Unpaired deep residual attributes learning for multi-domain face image translation," *IEEE Access*, vol. 7, pp. 132 594–132 608, 2019.
- [16] X. Mao, Q. Li, H. Xie, R. Y. Lau, Z. Wang, and S. Paul Smolley, "Least squares generative adversarial networks," in *Proceedings of the IEEE international conference on computer vision*, 2017, pp. 2794–2802.
- [17] S. Nowozin, B. Cseke, and R. Tomioka, "f-gan: Training generative neural samplers using variational divergence minimization," in *Advances in Neural Information Processing Systems*, 2016, pp. 271–279.
- [18] M. Arjovsky, S. Chintala, and L. Bottou, "Wasserstein gan," *arXiv preprint arXiv:1701.07875*, 2017.
- [19] L. Mescheder, S. Nowozin, and A. Geiger, "The numerics of gans," in *Advances in Neural Information Processing Systems*, 2017, pp. 1825–1835.
- [20] M. Heusel, H. Ramsauer, T. Unterthiner, B. Nessler, and S. Hochreiter, "Gans trained by a two time-scale update rule converge to a local nash equilibrium," *arXiv preprint arXiv:1706.08500*, 2017.
- [21] N. Kodali, J. Abernethy, J. Hays, and Z. Kira, "On convergence and stability of gans," *arXiv preprint arXiv:1705.07215*, 2017.
- [22] W. Nie and A. Patel, "Jr-gan: Jacobian regularization for generative adversarial networks," *arXiv preprint arXiv:1806.09235*, 2018.
- [23] A. Srivastava, L. Valkov, C. Russell, M. U. Gutmann, and C. Sutton, "Veegan: Reducing mode collapse in gans using implicit variational learning," in *Advances in Neural Information Processing Systems*, 2017, pp. 3308–3318.
- [24] M. Arjovsky and L. Bottou, "Towards principled methods for training generative adversarial networks," *Stat*, 2017.
- [25] Y. Yazici, C.-S. Foo, S. Winkler, K.-H. Yap, and V. Chandrasekhar, "Empirical analysis of overfitting and mode drop in gan training," in *2020 IEEE International Conference on Image Processing (ICIP)*. IEEE, 2020, pp. 1651–1655.
- [26] T. Chen, X. Zhai, M. Ritter, M. Lucic, and N. Houlsby, "Self-supervised gans via auxiliary rotation loss," in *Proceedings of the IEEE Conference on Computer Vision and Pattern Recognition*, 2019, pp. 12 154–12 163.
- [27] Y. Chen, G. Li, C. Jin, S. Liu, and T. Li, "Ssd-gan: Measuring the realness in the spatial and spectral domains," *arXiv preprint arXiv:2012.05535*, 2020.
- [28] K. Kurach, M. Lucic, X. Zhai, M. Michalski, and S. Gelly, "The gan landscape: Losses, architectures, regularization, and normalization," 2018.
- [29] T. Karras, T. Aila, S. Laine, and J. Lehtinen, "Progressive growing of gans for improved quality, stability, and variation," *arXiv preprint arXiv:1710.10196*, 2017.
- [30] A. Brock, J. Donahue, and K. Simonyan, "Large scale gan training for high fidelity natural image synthesis," *arXiv preprint arXiv:1809.11096*, 2018.
- [31] I. Gulrajani, F. Ahmed, M. Arjovsky, V. Dumoulin, and A. C. Courville, "Improved training of wasserstein gans," in *Advances in Neural Information Processing Systems*, 2017, pp. 5767–5777.
- [32] Z. Zhao, S. Singh, H. Lee, Z. Zhang, A. Odena, and H. Zhang, "Improved consistency regularization for gans," *arXiv preprint arXiv:2002.04724*, 2020.
- [33] T. Park and G. Casella, "The bayesian lasso," *Journal of the American Statistical Association*, vol. 103, no. 482, pp. 681–686, 2008.

- [34] A. E. Hoerl and R. W. Kennard, "Ridge regression: Biased estimation for nonorthogonal problems," *Technometrics*, vol. 12, no. 1, pp. 55–67, 1970.
- [35] R. G. Soares, H. Chen, and X. Yao, "Semisupervised classification with cluster regularization," *IEEE Transactions on Neural Networks and Learning Systems*, vol. 23, no. 11, pp. 1779–1792, 2012.
- [36] J. Hong, Y. Li, and H. Chen, "Variant grassmann manifolds: A representation augmentation method for action recognition," *ACM Transactions on Knowledge Discovery from Data (TKDD)*, vol. 13, no. 2, pp. 1–23, 2019.
- [37] H. Zhao, J. Zheng, W. Deng, and Y. Song, "Semi-supervised broad learning system based on manifold regularization and broad network," *IEEE Transactions on Circuits and Systems I: Regular Papers*, vol. 67, no. 3, pp. 983–994, 2020.
- [38] B. Jiang, C. Li, M. D. Rijke, X. Yao, and H. Chen, "Probabilistic feature selection and classification vector machine," *ACM Transactions on Knowledge Discovery from Data*, vol. 13, no. 2, pp. 1–27, 2019.
- [39] Z. Hu, F. Nie, R. Wang, and X. Li, "Low rank regularization: A review," *Neural Networks*, 2020.
- [40] S. Ioffe and C. Szegedy, "Batch normalization: Accelerating deep network training by reducing internal covariate shift," *arXiv preprint arXiv:1502.03167*, 2015.
- [41] J. L. Ba, J. R. Kiros, and G. E. Hinton, "Layer normalization," *arXiv preprint arXiv:1607.06450*, 2016.
- [42] L. Bottou, "Large-scale machine learning with stochastic gradient descent," in *Proceedings of International Conference on Computational Statistics*. Springer, 2010, pp. 177–186.
- [43] Y. Wu, P. Zhou, A. G. Wilson, E. P. Xing, and Z. Hu, "Improving gan training with probability ratio clipping and sample reweighting," *arXiv preprint arXiv:2006.06900*, 2020.
- [44] S. Zhao, H. Ren, A. Yuan, J. Song, N. Goodman, and S. Ermon, "Bias and generalization in deep generative models: An empirical study," *arXiv preprint arXiv:1811.03259*, 2018.
- [45] Z. Li, P. Xia, X. Rui, Y. Hu, and B. Li, "Are high-frequency components beneficial for training of generative adversarial networks," *arXiv preprint arXiv:2103.11093*, 2021.
- [46] T. Miyato, T. Kataoka, M. Koyama, and Y. Yoshida, "Spectral normalization for generative adversarial networks," *arXiv preprint arXiv:1802.05957*, 2018.
- [47] S. Zhao, Z. Liu, J. Lin, J.-Y. Zhu, and S. Han, "Differentiable augmentation for data-efficient gan training," *Advances in Neural Information Processing Systems*, vol. 33, 2020.
- [48] H. Zhang, Z. Zhang, A. Odena, and H. Lee, "Consistency regularization for generative adversarial networks," *arXiv preprint arXiv:1910.12027*, 2019.
- [49] H. Petzka, A. Fischer, and D. Lukovnikov, "On the regularization of wasserstein gans," *arXiv preprint arXiv:1709.08894*, 2017.
- [50] X. Wei, B. Gong, Z. Liu, W. Lu, and L. Wang, "Improving the improved training of wasserstein gans: A consistency term and its dual effect," *arXiv preprint arXiv:1803.01541*, 2018.
- [51] K. Kurach, M. Lucic, X. Zhai, M. Michalski, and S. Gelly, "A large-scale study on regularization and normalization in gans," *arXiv preprint arXiv:1807.04720*, 2018.
- [52] M. Lee and J. Seok, "Regularization methods for generative adversarial networks: An overview of recent studies," *arXiv preprint arXiv:2005.09165*, 2020.
- [53] A. Krogh and J. A. Hertz, "A simple weight decay can improve generalization," in *Advances in Neural Information Processing Systems*, 1992, pp. 950–957.
- [54] H. Chen, "Diversity and regularization in neural network ensembles," Ph.D. dissertation, University of Birmingham, 2008.
- [55] J. Kukačka, V. Golkov, and D. Cremers, "Regularization for deep learning: A taxonomy," *arXiv preprint arXiv:1710.10686*, 2017.
- [56] M. E. Tipping, "Sparse bayesian learning and the relevance vector machine," *Journal of Machine Learning Research*, vol. 1, no. Jun, pp. 211–244, 2001.
- [57] H. Chen, P. Tino, and X. Yao, "Probabilistic classification vector machines," *IEEE Transactions on Neural Networks*, vol. 20, no. 6, pp. 901–914, 2009.
- [58] H. Chen, P. Tiño, and X. Yao, "Efficient probabilistic classification vector machine with incremental basis function selection," *IEEE Transactions on Neural Networks and Learning Systems*, vol. 25, no. 2, pp. 356–369, 2013.
- [59] S. Lyu, X. Tian, Y. Li, B. Jiang, and H. Chen, "Multiclass probabilistic classification vector machine," *IEEE Transactions on Neural Networks and Learning Systems*, 2019.
- [60] H. Chen and X. Yao, "Regularized negative correlation learning for neural network ensembles," *IEEE Transactions on Neural Networks*, vol. 20, no. 12, pp. 1962–1979, 2009.
- [61] —, "Multiobjective neural network ensembles based on regularized negative correlation learning," *IEEE Transactions on Knowledge and Data Engineering*, vol. 22, no. 12, pp. 1738–1751, 2010.
- [62] J. Wen, X. Fang, Y. Xu, C. Tian, and L. Fei, "Low-rank representation with adaptive graph regularization," *Neural Networks*, vol. 108, pp. 83–96, 2018.
- [63] S. Zhou, F. Wang, Z. Huang, and J. Wang, "Discriminative feature learning with consistent attention regularization for person re-identification," in *Proceedings of the IEEE International Conference on Computer Vision*, 2019, pp. 8040–8049.
- [64] J. H. Lim and J. C. Ye, "Geometric gan," *arXiv preprint arXiv:1705.02894*, 2017.
- [65] K. Than and N. Vu, "Generalization of gans under lipschitz continuity and data augmentation," *arXiv preprint arXiv:2104.02388*, 2021.
- [66] J. Wu, Z. Huang, J. Thoma, D. Acharya, and L. Van Gool, "Wasserstein divergence for gans," in *Proceedings of the European Conference on Computer Vision*, 2018, pp. 653–668.
- [67] J. Su, "Gan-qp: A novel gan framework without gradient vanishing and lipschitz constraint," *arXiv preprint arXiv:1811.07296*, 2018.
- [68] N. Bonnefante, "From knothe's rearrangement to brenier's optimal transport map," *SIAM Journal on Mathematical Analysis*, vol. 45, no. 1, pp. 64–87, 2013.
- [69] L. V. Kantorovich, "On a problem of monge," *J. Math. Sci.(NY)*, vol. 133, p. 1383, 2006.
- [70] Y. Brenier, "Polar factorization and monotone rearrangement of vector-valued functions," *Communications on Pure and Applied Mathematics*, vol. 44, no. 4, pp. 375–417, 1991.
- [71] N. Lei, K. Su, L. Cui, S.-T. Yau, and X. D. Gu, "A geometric view of optimal transportation and generative model," *Computer Aided Geometric Design*, vol. 68, pp. 1–21, 2019.
- [72] G. Peyré, M. Cuturi et al., "Computational optimal transport," *Foundations and Trends in Machine Learning*, vol. 11, no. 5-6, pp. 355–607, 2019.
- [73] G. Huang, Z. Liu, L. van der Maaten, and K. Q. Weinberger, "Densely connected convolutional networks," in *Proceedings of the IEEE Conference on Computer Vision and Pattern Recognition*, July 2017.
- [74] K. He, X. Zhang, S. Ren, and J. Sun, "Deep residual learning for image recognition," in *Proceedings of the IEEE Conference on Computer Vision and Pattern Recognition*, 2016, pp. 770–778.
- [75] A. Yadav, S. Shah, Z. Xu, D. Jacobs, and T. Goldstein, "Stabilizing adversarial nets with prediction methods," *arXiv preprint arXiv:1705.07364*, 2017.
- [76] W. Nie and A. Patel, "Towards a better understanding and regularization of gan training dynamics," *arXiv preprint arXiv:1806.09235*, 2019.
- [77] J. Li, A. Madry, J. Peebles, and L. Schmidt, "On the limitations of first-order approximation in gan dynamics," *arXiv preprint arXiv:1706.09884*, 2017.
- [78] O. L. Mangasarian, *Nonlinear programming*. SIAM, 1994.
- [79] V. Nagarajan and J. Z. Kolter, "Gradient descent gan optimization is locally stable," in *Advances in Neural Information Processing Systems*, 2017, pp. 5585–5595.
- [80] L. Mescheder, A. Geiger, and S. Nowozin, "Which training methods for gans do actually converge?" *arXiv preprint arXiv:1801.04406*, 2018.
- [81] K. Roth, A. Lucchi, S. Nowozin, and T. Hofmann, "Stabilizing training of generative adversarial networks through regularization," in *Advances in Neural Information Processing Systems*, 2017, pp. 2018–2028.
- [82] G. Gidel, H. Berard, G. Vignoud, P. Vincent, and S. Lacoste-Julien, "A variational inequality perspective on generative adversarial networks," *arXiv preprint arXiv:1802.10551*, 2018.
- [83] M. Arjovsky and L. Bottou, "Towards principled methods for training generative adversarial networks," 2017.
- [84] J. Stanczuk, C. Etmann, L. M. Kreusser, and C.-B. Schönlieb, "Wasserstein gans work because they fail (to approximate the wasserstein distance)," *arXiv preprint arXiv:2103.01678*, 2021.
- [85] W. Fedus, M. Rosca, B. Lakshminarayanan, A. M. Dai, S. Mohamed, and I. Goodfellow, "Many paths to equilibrium: Gans do not need to decrease a divergence at every step," *arXiv preprint arXiv:1710.08446*, 2017.
- [86] Z. Zhou, J. Shen, Y. Song, W. Zhang, and Y. Yu, "Towards efficient and unbiased implementation of lipschitz continuity in gans," *arXiv preprint arXiv:1904.01184*, 2019.
- [87] D. Terjék, "Virtual adversarial lipschitz regularization," *arXiv preprint arXiv:1907.05681*, 2019.

- [88] J. Adler and S. Lunz, “Banach wasserstein gan,” in *Advances in Neural Information Processing Systems*, 2018, pp. 6754–6763.
- [89] M. Xu, Z. Zhou, G. Lu, J. Tang, W. Zhang, and Y. Yu, “Towards generalized implementation of wasserstein distance in gans,” 2021.
- [90] L. Zhang, Y. Zhang, and Y. Gao, “A wasserstein gan model with the total variational regularization,” *arXiv preprint arXiv:1812.00810*, 2018.
- [91] Z. Zhou, J. Liang, Y. Song, L. Yu, H. Wang, W. Zhang, Y. Yu, and Z. Zhang, “Lipschitz generative adversarial nets,” *arXiv preprint arXiv:1902.05687*, 2019.
- [92] H. Thanh-Tung, T. Tran, and S. Venkatesh, “Improving generalization and stability of generative adversarial networks,” *arXiv preprint arXiv:1902.03984*, 2019.
- [93] A. Mallasto, G. Montúfar, and A. Gerolin, “How well do wgens estimate the wasserstein metric?” *arXiv preprint arXiv:1910.03875*, 2019.
- [94] G.-J. Qi, “Loss-sensitive generative adversarial networks on lipschitz densities,” *International Journal of Computer Vision*, vol. 128, no. 5, pp. 1118–1140, 2020.
- [95] T. Miyato, S.-i. Maeda, M. Koyama, and S. Ishii, “Virtual adversarial training: a regularization method for supervised and semi-supervised learning,” *IEEE Transactions on Pattern Analysis and Machine Intelligence*, vol. 41, no. 8, pp. 1979–1993, 2018.
- [96] L. C. Evans, “Partial differential equations and monge-kantorovich mass transfer,” *Current developments in mathematics*, vol. 1997, no. 1, pp. 65–126, 1997.
- [97] T. Salimans, I. Goodfellow, W. Zaremba, V. Cheung, A. Radford, and X. Chen, “Improved techniques for training gans,” in *Advances in Neural Information Processing Systems*, 2016, pp. 2234–2242.
- [98] S. Barratt and R. Sharma, “A note on the inception score,” *arXiv preprint arXiv:1801.01973*, 2018.
- [99] Z. Zhang, Y. Zeng, L. Bai, Y. Hu, M. Wu, S. Wang, and E. R. Hancock, “Spectral bounding: Strictly satisfying the 1-lipschitz property for generative adversarial networks,” *Pattern Recognition*, p. 107179, 2019.
- [100] K. Liu, W. Tang, F. Zhou, and G. Qiu, “Spectral regularization for combating mode collapse in gans,” in *Proceedings of the IEEE International Conference on Computer Vision*, 2019, pp. 6382–6390.
- [101] R. Mathias, “The spectral norm of a nonnegative matrix,” *Linear Algebra and its Applications*, vol. 139, pp. 269–284, 1990.
- [102] C. Zhou, J. Zhang, and J. Liu, “Lp-wgan: Using lp-norm normalization to stabilize wasserstein generative adversarial networks,” *Knowledge-Based Systems*, vol. 161, pp. 415–424, 2018.
- [103] A. Krizhevsky, I. Sutskever, and G. E. Hinton, “Imagenet classification with deep convolutional neural networks,” *Communications of the ACM*, vol. 60, no. 6, pp. 84–90, 2017.
- [104] L. Wan, M. Zeiler, S. Zhang, Y. Le Cun, and R. Fergus, “Regularization of neural networks using dropconnect,” in *International conference on machine learning*, 2013, pp. 1058–1066.
- [105] T. DeVries and G. W. Taylor, “Improved regularization of convolutional neural networks with cutout,” *arXiv preprint arXiv:1708.04552*, 2017.
- [106] S. Yun, D. Han, S. J. Oh, S. Chun, J. Choe, and Y. Yoo, “Cutmix: Regularization strategy to train strong classifiers with localizable features,” in *Proceedings of the IEEE International Conference on Computer Vision*, 2019, pp. 6023–6032.
- [107] H. Zhang, M. Cisse, Y. N. Dauphin, and D. Lopez-Paz, “mixup: Beyond empirical risk minimization,” *arXiv preprint arXiv:1710.09412*, 2017.
- [108] H.-Y. Tseng, L. Jiang, C. Liu, M.-H. Yang, and W. Yang, “Regularizing generative adversarial networks under limited data,” *arXiv preprint arXiv:2104.03310*, 2021.
- [109] Z. Zhao, Z. Zhang, T. Chen, S. Singh, and H. Zhang, “Image augmentations for gan training,” *arXiv preprint arXiv:2006.02595*, 2020.
- [110] T. Karras, M. Aittala, J. Hellsten, S. Laine, J. Lehtinen, and T. Aila, “Training generative adversarial networks with limited data,” *Advances in Neural Information Processing Systems*, vol. 33, 2020.
- [111] N.-T. Tran, V.-H. Tran, N.-B. Nguyen, T.-K. Nguyen, and N.-M. Cheung, “Towards good practices for data augmentation in gan training,” *arXiv preprint arXiv:2006.05338*, 2020.
- [112] J. Jeong and J. Shin, “Training gans with stronger augmentations via contrastive discriminator,” 2021.
- [113] I. Anokhin, K. Demochkin, T. Khakhulin, G. Sterkin, V. Lempitsky, and D. Korzhennikov, “Image generators with conditionally-independent pixel synthesis,” 2020.
- [114] Q. Xie, Z. Dai, E. Hovy, M.-T. Luong, and Q. V. Le, “Unsupervised data augmentation for consistency training,” *arXiv preprint arXiv:1904.12848*, 2019.
- [115] K. Sohn, D. Berthelot, C.-L. Li, Z. Zhang, N. Carlini, E. D. Cubuk, A. Kurakin, H. Zhang, and C. Raffel, “Fixmatch: Simplifying semi-supervised learning with consistency and confidence,” *arXiv preprint arXiv:2001.07685*, 2020.
- [116] M. Gao, Z. Zhang, G. Yu, S. O. Arik, L. S. Davis, and T. Pfister, “Consistency-based semi-supervised active learning: Towards minimizing labeling cost,” *arXiv preprint arXiv:1910.07153*, 2019.
- [117] T. Chen, S. Kornblith, M. Norouzi, and G. Hinton, “A simple framework for contrastive learning of visual representations,” in *International conference on machine learning*. PMLR, 2020, pp. 1597–1607.
- [118] A. Jolicoeur-Martineau, “The relativistic discriminator: a key element missing from standard gan,” *arXiv preprint arXiv:1807.00734*, 2018.
- [119] J. Su, “Training generative adversarial networks via turing test,” *arXiv preprint arXiv:1810.10948*, 2018.
- [120] Y. Xiangli, Y. Deng, B. Dai, C. C. Loy, and D. Lin, “Real or not real, that is the question,” *arXiv preprint arXiv:2002.05512*, 2020.
- [121] Y.-G. Shin, Y.-J. Yeo, and S.-J. Ko, “Simple yet effective way for improving the performance of gan,” *arXiv preprint arXiv:1911.10979*, 2019.
- [122] Y. Mroueh, T. Sercu, and V. Goel, “Mcgan: Mean and covariance feature matching gan,” *arXiv preprint arXiv:1702.08398*, 2017.
- [123] R. Durall, M. Keuper, and J. Keuper, “Watch your up-convolution: Cnn based generative deep neural networks are failing to reproduce spectral distributions,” in *Proceedings of the IEEE/CVF Conference on Computer Vision and Pattern Recognition*, 2020, pp. 7890–7899.
- [124] T. Ohkawa, N. Inoue, H. Kataoka, and N. Inoue, “Augmented cyclic consistency regularization for unpaired image-to-image translation,” *arXiv preprint arXiv:2003.00187*, 2020.
- [125] K. He, H. Fan, Y. Wu, S. Xie, and R. Girshick, “Momentum contrast for unsupervised visual representation learning,” in *Proceedings of the IEEE/CVF Conference on Computer Vision and Pattern Recognition*, 2020, pp. 9729–9738.
- [126] R. D. Hjelm, A. Fedorov, S. Lavoie-Marchildon, K. Grewal, P. Bachman, A. Trischler, and Y. Bengio, “Learning deep representations by mutual information estimation and maximization,” *arXiv preprint arXiv:1808.06670*, 2018.
- [127] C. Doersch, A. Gupta, and A. A. Efros, “Unsupervised visual representation learning by context prediction,” in *Proceedings of the IEEE International Conference on Computer Vision*, 2015, pp. 1422–1430.
- [128] S. Gidaris, P. Singh, and N. Komodakis, “Unsupervised representation learning by predicting image rotations,” *arXiv preprint arXiv:1803.07728*, 2018.
- [129] H. Lee, S. J. Hwang, and J. Shin, “Rethinking data augmentation: Self-supervision and self-distillation,” *arXiv preprint arXiv:1910.05872*, 2019.
- [130] A. Kolesnikov, X. Zhai, and L. Beyer, “Revisiting self-supervised visual representation learning,” in *Proceedings of the IEEE Conference on Computer Vision and Pattern Recognition*, 2019, pp. 1920–1929.
- [131] X. Zhai, A. Oliver, A. Kolesnikov, and L. Beyer, “S4l: Self-supervised semi-supervised learning,” in *Proceedings of the IEEE International Conference on Computer Vision*, 2019, pp. 1476–1485.
- [132] R. Huang, W. Xu, T.-Y. Lee, A. Cherian, Y. Wang, and T. Marks, “Fxxgan: Self-supervised gan learning via feature exchange,” in *Proceedings of the IEEE Winter Conference on Applications of Computer Vision*, 2020, pp. 3194–3202.
- [133] G. Baykal and G. Unal, “DeshuffleGAN: A self-supervised gan to improve structure learning,” *arXiv preprint arXiv:2006.08694*, 2020.
- [134] P. Patel, N. Kumari, M. Singh, and B. Krishnamurthy, “Lt-gan: Self-supervised gan with latent transformation detection,” in *Proceedings of the IEEE/CVF Winter Conference on Applications of Computer Vision*, 2021, pp. 3189–3198.
- [135] F. M. Carlucci, A. D’Innocente, S. Bucci, B. Caputo, and T. Tommasi, “Domain generalization by solving jigsaw puzzles,” in *Proceedings of the IEEE Conference on Computer Vision and Pattern Recognition*, 2019, pp. 2229–2238.
- [136] N.-T. Tran, V.-H. Tran, B.-N. Nguyen, L. Yang *et al.*, “Self-supervised gan: Analysis and improvement with multi-class minimax game,” in *Advances in Neural Information Processing Systems*, 2019, pp. 13 253–13 264.
- [137] K. S. Lee, N.-T. Tran, and N.-M. Cheung, “Infomax-gan: Improved adversarial image generation via information maximization and contrastive learning,” *arXiv preprint arXiv:2007.04589*, 2020.
- [138] A. v. d. Oord, Y. Li, and O. Vinyals, “Representation learning with contrastive predictive coding,” *arXiv preprint arXiv:1807.03748*, 2018.
- [139] R. D. Hjelm, A. Fedorov, S. Lavoie-Marchildon, K. Grewal, P. Bachman, A. Trischler, and Y. Bengio, “Learning deep representations by mutual information estimation and maximization,” 2019.

- [140] D. Ulyanov, A. Vedaldi, and V. Lempitsky, "Instance normalization: The missing ingredient for fast stylization," *arXiv preprint arXiv:1607.08022*, 2016.
- [141] Y. Wu and K. He, "Group normalization," in *Proceedings of the European conference on computer vision (ECCV)*, 2018, pp. 3–19.
- [142] T. Salimans and D. P. Kingma, "Weight normalization: A simple reparameterization to accelerate training of deep neural networks," in *Advances in Neural Information Processing Systems*, 2016, pp. 901–909.
- [143] T. Miyato and M. Koyama, "cgans with projection discriminator," *arXiv preprint arXiv:1802.05637*, 2018.
- [144] H. Zhang, I. Goodfellow, D. Metaxas, and A. Odena, "Self-attention generative adversarial networks," *arXiv preprint arXiv:1805.08318*, 2018.
- [145] X. Huang and S. Belongie, "Arbitrary style transfer in real-time with adaptive instance normalization," in *Proceedings of the IEEE International Conference on Computer Vision*, 2017, pp. 1501–1510.
- [146] T. Karras, S. Laine, and T. Aila, "A style-based generator architecture for generative adversarial networks," in *Proceedings of the IEEE Conference on Computer Vision and Pattern Recognition*, 2019, pp. 4401–4410.
- [147] T. Park, M.-Y. Liu, T.-C. Wang, and J.-Y. Zhu, "Semantic image synthesis with spatially-adaptive normalization," in *Proceedings of the IEEE Conference on Computer Vision and Pattern Recognition*, 2019, pp. 2337–2346.
- [148] Y. Wang, Y.-C. Chen, X. Zhang, J. Sun, and J. Jia, "Attentive normalization for conditional image generation," in *Proceedings of the IEEE/CVF Conference on Computer Vision and Pattern Recognition*, 2020, pp. 5094–5103.
- [149] S. Xiang and H. Li, "On the effects of batch and weight normalization in generative adversarial networks," *arXiv preprint arXiv:1704.03971*, 2017.
- [150] D. Yang, S. Hong, Y. Jang, T. Zhao, and H. Lee, "Diversity-sensitive conditional generative adversarial networks," *arXiv preprint arXiv:1901.09024*, 2019.
- [151] A. Odena, J. Buckman, C. Olsson, T. B. Brown, C. Olah, C. Raffel, and I. Goodfellow, "Is generator conditioning causally related to gan performance?" *arXiv preprint arXiv:1802.08768*, 2018.
- [152] X. Gong, S. Chang, Y. Jiang, and Z. Wang, "Autogan: Neural architecture search for generative adversarial networks," in *Proceedings of the IEEE/CVF International Conference on Computer Vision*, 2019, pp. 3224–3234.
- [153] T. Karras, S. Laine, M. Aittala, J. Hellsten, J. Lehtinen, and T. Aila, "Analyzing and improving the image quality of stylegan," in *Proceedings of the IEEE/CVF Conference on Computer Vision and Pattern Recognition*, 2020, pp. 8110–8119.
- [154] S. Zhao, J. Cui, Y. Sheng, Y. Dong, X. Liang, E. I. Chang, and Y. Xu, "Large scale image completion via co-modulated generative adversarial networks," *arXiv preprint arXiv:2103.10428*, 2021.
- [155] E. Richardson, Y. Alaluf, O. Patashnik, Y. Nitzan, Y. Azar, S. Shapiro, and D. Cohen-Or, "Encoding in style: a stylegan encoder for image-to-image translation," *arXiv preprint arXiv:2008.00951*, 2020.



Ziqiang Li received the B.E. degree from University of Science and Technology of China (USTC), Hefei, China, in 2019 and is pursuing the Master degree from University of Science and Technology of China (USTC), Hefei, China. His research interests include medical image segmentation, deep generative models and machine learning.



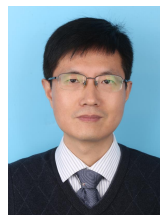
Rentuo Tao received the B.E. degree from Hefei University of Technology (HFUT), Hefei, China, in 2013 and is pursuing the Ph.D. degree from University of Science and Technology of China (USTC), Hefei, China. His research interests include deep generative models, machine learning and computer vision.



Pengfei Xia received the B.E. degree from the China University of Mining and Technology (CUMT), XuZhou, China, in 2015. He is currently pursuing the Ph.D. degree with the University of Science and Technology of China (USTC), Hefei, China. His research interests including adversarial examples and deep learning security.



Huanhuan Chen (M'09–SM'16) received the B.Sc. degree from the University of Science and Technology of China (USTC), Hefei, China, in 2004, and the Ph.D. degree in computer science from the University of Birmingham, Birmingham, U.K., in 2008. He is currently a Full Professor with the School of Computer Science and Technology, USTC. His current research interests include neural networks, Bayesian inference, and evolutionary computation. Dr. Chen was a recipient of the 2015 International Neural Network Society Young Investigator Award, the 2012 IEEE Computational Intelligence Society Outstanding Ph.D. Dissertation Award, the IEEE TRANSACTIONS ON NEURAL NETWORKS Outstanding Paper Award (bestowed in 2012 and only one article in 2009), and the 2009 British Computer Society Distinguished Dissertations Award. He serves as an Associate Editor for the IEEE TRANSACTIONS ON NEURAL NETWORKS AND LEARNING SYSTEMS and the IEEE TRANSACTIONS ON EMERGING TOPICS IN COMPUTATIONAL INTELLIGENCE.



Bin Li received the B.Sc. degree from the Hefei University of Technology, Hefei, China, in 1992, the M.Sc. degree from the Institute of Plasma Physics, Chinese Academy of Sciences, Hefei, in 1995, and the Ph.D. degree from the University of Science and Technology of China (USTC), Hefei, in 2001. He is currently a Professor with the School of Information Science and Technology, USTC. He has authored or co-authored over 40 refereed publications. His current research interests include evolutionary computation, pattern recognition, and human-computer interaction. Dr. Li is the Founding Chair of the IEEE Computational Intelligence Society Hefei Chapter, a Counselor of the IEEE USTC Student Branch, a Senior Member of the Chinese Institute of Electronics (CIE), and a member of the Technical Committee of the Electronic Circuits and Systems Section of CIE.